



Published in final edited form as:

Nature. 2015 July 16; 523(7560): 342–346. doi:10.1038/nature14462.

HDL-bound sphingosine 1-phosphate restrains lymphopoiesis and neuroinflammation

Victoria A. Blaho^{1,2}, Sylvain Galvani¹, Eric Engelbrecht¹, Catherine Liu¹, Steven L. Swendeman¹, Mari Kono³, Richard L. Proia³, Lawrence Steinman⁴, May H. Han⁴, and Timothy Hla^{1,2,*}

¹Center for Vascular Biology, Department of Pathology and Laboratory Medicine

²Brain and Mind Research Institute, Weill Medical College of Cornell University, New York, NY 10065, USA

³Genetics of Development and Disease Branch, National Institute of Diabetes and Digestive and Kidney Diseases, NIH, Bethesda, Maryland, USA

⁴Department of Neurology and Neurological Sciences, Stanford University, Stanford, CA 94305, USA

Summary

Lipid mediators influence immunity in myriad ways. For example, circulating sphingosine 1-phosphate (S1P) is a key regulator of lymphocyte egress^{1,2}. Although the majority of plasma S1P is bound to apolipoprotein M (ApoM) in the high-density lipoprotein (HDL) particle³, immunological functions of the ApoM-S1P complex are unknown. Here, we show that ApoM-S1P is dispensable for lymphocyte trafficking yet restrains lymphopoiesis by activating the S1P₁ receptor on bone marrow (BM) lymphocyte progenitors. Mice that lacked ApoM (*Apom*^{-/-}) had increased proliferation of Lin⁻Sca1⁺cKit⁺ hematopoietic progenitor cells (LSK) and common lymphoid progenitors (CLP) in BM. Pharmacologic activation or genetic overexpression of S1P₁ suppressed LSK and CLP proliferation *in vivo*. ApoM was stably associated with BM CLPs, which showed active S1P₁ signaling *in vivo*⁴. Moreover, ApoM⁺HDL, but not albumin-bound S1P, inhibited lymphopoiesis *in vitro*. Upon immune stimulation, *Apom*^{-/-} mice developed more severe experimental autoimmune encephalomyelitis⁵, characterized by increased lymphocytes in the central nervous system (CNS) and breakdown of the blood-brain barrier. Thus, the ApoM-S1P-S1P₁ signaling axis restrains the lymphocyte compartment and subsequently, adaptive immune responses. Unique biological functions imparted by specific S1P chaperones could be exploited for novel therapeutic opportunities.

Reprints and permissions information is available at www.nature.com/reprints.

*Correspondence and requests for materials should be addressed to T.H. (tih2002@med.cornell.edu).

Author contributions

V.A.B. designed and performed the experiments, analyzed and interpreted data, and wrote the manuscript. S.G., E.E., C.L., and S.S. performed experiments and analyzed data. Y.H., L.S., and M.H.H. contributed to EAE studies. R.L.P. and M.K. contributed to the reporter mice studies. T.H. supervised the overall project, designed experiments, interpreted data, and wrote the manuscript. All authors read and commented on the manuscript.

The authors declare no competing financial interests.

Sphingosine 1-phosphate (S1P), a bioactive lysophospholipid mediator, interacts with vertebrate-specific S1P receptors to regulate various physiological functions⁶. Most cells express one or more of the G protein-coupled S1P receptors (S1P₁₋₅), which mediate cellular responses such as cell migration, adhesion, and survival⁷. A unique feature of this signaling system is the enrichment of the ligand, S1P, in lymph and blood compared to interstitial fluids^{1,2}. The majority (~65%) of plasma S1P is complexed with apolipoprotein M (ApoM), whereas the remainder is found in the lipoprotein-free fraction, presumably associated with albumin⁴. Circulating ApoM is predominantly associated with a specific population of HDL particles (ApoM⁺HDL)^{8,9}. S1P bound to ApoM⁺HDL maintains pulmonary vascular barrier function and migration of endothelial cells *in vitro*^{3,10}.

Activation of S1P₁ receptor on immune cells residing in secondary lymphoid organs and thymus is critical for lymphocyte egress into circulation^{1,2,11}. FTY720 (Fingolimod, GilenyaTM), the first oral treatment for relapsing-remitting multiple sclerosis (RRMS), targets this pathway, inducing lymphopenia and diminishing infiltration of autoreactive lymphocytes into the central nervous system (CNS)¹². Emerging evidence indicates that S1P₁ also regulates T cell differentiation, including T helper 17 (T_H17) and T helper 1 (T_H1) / T_{reg} balance^{13,14}. However, the role of S1P signaling in lymphocyte development, homeostasis, and activation remain unclear. Additionally, given the poor aqueous solubility of S1P, it is unknown whether chaperones impart specificity to S1P signals in lymphocytes, resulting in distinct immune responses.

We determined if ApoM levels affected the S1P concentrations in blood and lymph, which are known to be important for lymphocyte egress. Although plasma S1P was decreased by ~60%³, lymph S1P concentrations were not changed in *Apom*^{-/-} mice (Extended Data Fig. 1a). ApoM in lymph was estimated to be approximately half of plasma levels (Extended Data Fig. 1b). Albumin concentrations in blood and lymph were similar between WT and *Apom*^{-/-} mice (Extended Data Fig. 1c). Analysis of peripheral blood revealed a surprising increase of CD4⁺ and CD8⁺ T cells and CD19⁺ B cells in *Apom*^{-/-} mice (Fig. 1a), whereas circulating monocyte and neutrophil numbers were similar. Numbers of CD4, CD8, and CD19 cells were also increased in lymph (Fig. 1b). Lymphocytosis was not caused by a loss of endothelial cell S1P₁ signaling, since inducible endothelial cell-specific deletion of *S1pr1* (S1P₁ ECKO)¹⁵ did not affect blood lymphocyte numbers (Extended Data Fig. 1d). In contrast, global knockout of *S1pr1* resulted in severe lymphopenia, consistent with a requirement for S1P₁ in lymphocyte egress from secondary lymphoid organs (SLO) and thymus (Extended Data Fig. 1d)¹. While examination of lymph nodes (brachial and inguinal) revealed similar lymphocyte numbers in *Apom*^{-/-} mice compared to WT (Extended Data Fig 2a), thymi of *Apom*^{-/-} mice contained significantly more CD4⁺CD8⁺ double positive (DP) and CD4⁺ or CD8⁺ single positive (SP) cells (Extended Data Fig 2b). B cell populations in spleens of *Apom*^{-/-} mice were slightly increased but there were no differences in the T cell populations or spleen weights (Extended Data Fig 2c, d). Surface expression of lymphocyte activation markers CD69 and CD62L were unchanged in the LN, thymus or spleen (Extended Data Fig 3a-c). Administration of anti-integrin antibodies, which block lymphocyte entry into lymph nodes, had similar effects on WT and *Apom*^{-/-}

lymph node cell numbers (Extended Data Fig 3d), implying that ApoM⁺HDL is not critical for lymphocyte egress.

FTY720, which induces internalization of S1P₁, induces lymphopenia^{1,12}. In both WT and *Apom*^{-/-} mice, administration of FTY720 resulted in marked lymphopenia in blood and lymph 2h post-administration, with similar retention patterns of increased CD4, CD8, and CD19 cells in LN and spleen (Extended Data Fig. 4 a-d). Double negative (DN) thymocytes were decreased whereas DP and SP cells increased in thymi of both WT and *Apom*^{-/-} mice (Extended Data Fig. 4e). Similar degree of lymphopenia was seen using two S1P₁-selective agonists, AUY954 and SEW2871 (Extended Data Fig. 4f, g)^{16,17}. Collectively, these data suggest that lymphocyte trafficking out of thymus and SLO into blood and lymph is not dependent on ApoM⁺HDL.

To determine the cause of lymphocytosis seen in *Apom*^{-/-} mice, we examined hematopoietic cell populations in blood and BM (Extended Data Fig. 5a-c). Lin⁻Sca1⁺cKit⁺ (LSK) cells, a designation encompassing several distinct hematopoietic stem and progenitor populations, were more abundant in blood and BM of *Apom*^{-/-} mice (Fig. 1c). BM of *Apom*^{-/-} mice also contained increased numbers of common lymphoid progenitors (CLP; Lin⁻Flt3⁺IL7Rα⁺cKit⁺) whereas granulocyte macrophage progenitors (GMP; LKSca-1⁻CD34⁺FcγRII/III^{hi}), common myeloid progenitors (CMP; LKSca-1⁻CD34⁺FcγRII/III^{lo/-}), and megakaryocyte/erythrocyte progenitors (MEP; LKSca-1⁻CD34⁺FcγRII/III^{lo/-}) were unchanged (Fig. 1d)¹⁸⁻²⁰. Pre-, immature, and mature B cells in the BM (Fig. 1e) and early thymic progenitors (ETP) / double negative 1 (DN1; CD4⁻CD8⁻CD3⁻cKit⁺CD44⁺CD25⁻) in the thymus were increased in *Apom*^{-/-} mice (Fig. 1f). Although S1P may have a role in LSK recirculation from tissues to BM¹⁹, B cell BM egress, which is insensitive to pertussis toxin, is likely not involved in the lymphocytosis seen in *Apom*^{-/-} mice²¹. 2.5 hours after bromodeoxyuridine (BrdU) injection, *Apom*^{-/-} LSK and CLP had significantly more BrdU incorporation compared to WT cells (Fig. 1g; Extended Data Fig. 5d). No measurable difference was detected in myeloid progenitors. Cell cycle analysis demonstrated increased fractions of LSK and CLP, but not LKS⁻, in S/G2/M phase in *Apom*^{-/-} BM (Fig. 1h, i)¹⁸. These data suggested that ApoM restrained cell cycle entry specifically in BM progenitors destined for lymphoid lineages.

Genetic deletion of the cholesterol transporters ATP-binding cassette (ABC) ABCA1 and ABCG1, which interact with HDL to export cellular cholesterol, results in significant increases in LSK and myeloid progenitor cells^{18,22}. ABCG1 single knockout²³ or deletion of scavenger receptor (SR)-B1²⁴, a high-affinity HDL receptor, resulted in increased mature T or B cell, respectively, while not affecting their progenitors. Our findings suggested a BM compartment-specific function of ApoM⁺HDL in lymphocyte ontogeny. We next investigated whether IL-7, a key regulator of lymphopoiesis²⁰, was influenced by ApoM-S1P signaling. IL-7 concentrations in the BM (Extended Data Fig. 5e) and CLP IL-7Rα surface expression (Extended Data Fig. 5f) were similar between WT and *Apom*^{-/-} mice. Thus, modulation of the IL-7 / IL-7Rα interaction is unlikely to be responsible for ApoM-mediated suppression of lymphopoiesis.

To examine the role of S1P in progenitor proliferation regulated by ApoM⁺HDL, WT and *Apom*^{-/-} mice were treated with SEW2871 and BM cell BrdU incorporation examined (Fig. 2a). SEW2871 treatment suppressed BrdU incorporation in *Apom*^{-/-} LSK and CLP but not in WT counterparts. Treatment with AUY954 or FTY720 also had similar effects (Extended Data Fig 6a, b), suggesting that pharmacologic activation of S1P₁ on LSK and CLP suppresses their proliferation. We next determined LSK and CLP numbers in BM of mice with an inducible *S1pr1* transgene (*S1pr1* OE; Extended Data Fig. 7a-c)¹⁵. Induction of S1P₁ expression led to decreased numbers of LSK and CLP (Fig. 2b). Blood LSK numbers were also reduced, ruling out increased BM egress of hematopoietic progenitors (Fig. 2c). Both LSK and CLP populations showed decreased BrdU incorporation (Fig. 2d). S1P₁ overexpression also resulted in decreased ETP in thymus (Fig. 2e). Mature T and B cell numbers in blood were unchanged and SLO had reduced cell numbers (Fig. 2f; Extended Data Fig 7d-f), suggesting increased egress of mature lymphocytes from lymphoid organs upon S1P₁ overexpression. These pharmacologic and genetic data further confirm that ApoM⁺HDL signaling via BM progenitor cell S1P₁ restrains lymphopoiesis.

Real-time RT-PCR analysis found that *S1pr1* mRNA is expressed by CLP and confirmed a previous report of its expression by LSK (Extended Data Fig. 8a)¹⁹. Immunofluorescence analysis of Lin⁻ Sca1⁺ BM cells from WT mice showed stable association of ApoM with the cell surface (Fig. 2g). To determine if S1P₁ is active in BM progenitor cells *in vivo*, we used S1P₁ GFP signaling mice, which show nuclear GFP signal upon receptor activation (Extended Data Fig. 8b-f)⁴ and found that CLP and LSK show active S1P₁ signaling (Fig. 2h,i).

We next examined the signal transducer and activator of transcription 5 (Stat5) pathway, which is activated by IL-7R signaling and regulates lymphocyte development, proliferation, and differentiation^{25,26}. Phosphoflow analysis (Extended Data Fig. 8g, h) revealed significantly increased phospho-Stat5 in *Apom*^{-/-} CLP compared to WT cells (Fig. 2j). Conversely, extracellular signal-regulated kinases 1 and 2 (Erk1/2) antagonizes the proliferative signals induced by Stat5²⁶. CLP from mice lacking ApoM-S1P had significantly less phospho-Erk1/2 than WT CLP (Fig. 2k). Collectively, these data suggest that ApoM-S1P directly interacts with BM lymphocyte progenitors and activates the S1P₁/ERK pathway to restrain their proliferation.

To test if ApoM⁺HDL modulated lymphocyte development directly, we utilized *in vitro* lymphopoiesis assays. Using Lin⁻ cells from WT BM, we observed that the generation of B220⁺ cells (pre-, pro-, and immature B lymphocytes) was strongly suppressed by ApoM⁺HDL but not by albumin-bound S1P (Fig 3a,b; Extended Data Fig 9a). HDL from *Apom*^{-/-} mice, which lacks S1P (ApoM⁻HDL) (Extended Data Fig 9b) did not suppress lymphopoiesis (Fig. 3c). ApoM⁺HDL-mediated suppression of lymphopoiesis was blocked by preincubation of HDL with an anti-S1P IgM²⁸ but not by an irrelevant IgM (Fig. 3d). These findings suggest that ApoM⁺HDL-bound S1P is critical to restrain lymphocyte progenitor differentiation and proliferation.

To determine the involvement of S1P₁, cultures were incubated with AUY954 or phosphorylated FTY720 (FTY720p), resulting in significantly decreased numbers of B220⁺

cells (Fig. 3e). However, incubation of Lin⁻ BM cells with W146, a selective S1P₁ antagonist, abrogated the suppressive effect of ApoM⁺HDL. Next, we used Lin⁻ BM from S1P^{S5A}₁ mice, which express a mutated S1P₁ that is internalization defective, resulting in extended surface residency and sustained signaling^{13,17,27}. S1P^{S5A}₁ BM cells were more sensitive to ApoM-S1P than WT BM, since lower S1P concentrations were sufficient to repress B220⁺ development (Fig. 3f). Despite greater S1P sensitivity, albumin-S1P was unable to suppress lymphopoiesis by S1P^{S5A}₁ cells, similar to WT cells. ApoM⁻HDL did not suppress B220⁺ generation from S1P^{S5A}₁ BM cells (Fig. 3g). Collectively, these findings support the hypothesis that ApoM⁺HDL activation of S1P₁ on lymphocyte progenitors inhibits their proliferation.

We hypothesized that modulation of lymphocyte compartment size by ApoM⁺HDL could impact the magnitude of immune responses. The experimental autoimmune encephalomyelitis (EAE) model recapitulates many aspects of multiple sclerosis (MS) pathology, including increased BM cell proliferative capacity, blood brain barrier (BBB) disruption, and autoreactive immune cell CNS infiltration⁵. Interestingly, increased plasma HDL correlates with decreased acute inflammation in MS patients, although the mechanism and the role of specific HDL populations are unknown^{28,29}. To ascertain whether the expanded lymphocyte compartment in *Apom*^{-/-} mice could affect the extent and intensity of the adaptive immune response, we induced EAE in WT, *Apom*^{-/-} mice, and mice overexpressing a human ApoM transgene (*Apom*^{Tg})³ by immunization with myelin oligoglycoprotein (MOG₃₅₋₅₅) peptide. Mice lacking ApoM developed symptoms earlier and exhibited more severe CNS pathology compared to WT mice (Figure 4a). Remarkably, *Apom*^{Tg} mice developed milder symptoms, supporting a protective role for ApoM-S1P (Figure 4a). More severe inflammation in the CNS was evident at day 16 post-immunization in *Apom*^{-/-} brains as compared to WT counterparts (Figure 4b) and increased lymphocytes were found in *Apom*^{-/-} brains at the peak of disease (Figure 4c) Lymphocytes from MOG-immunized *Apom*^{-/-} mice were highly activated, as demonstrated by increased splenocyte proliferative responses to ex vivo MOG restimulation (Figure 4d). Thus, the increase in BM proliferation of lymphocyte progenitors and increased circulating lymphocytes in *Apom*^{-/-} mice resulted in an exaggerated autoimmune neuroinflammatory response, whereas overexpression of ApoM was protective.

Previously, our laboratory has reported that the loss of ApoM results in enhanced pulmonary vascular leakage³. To determine if altered vascular barrier function was contributing to increased EAE severity, WT and *Apom*^{-/-} mice were injected intravenously with tetramethylrhodamine (TMR)-labeled dextran (70 kD) before or eight days post-MOG₃₅₋₅₅ immunization to assess BBB functionality. Before immunization, no differences in dextran extravasation were evident in brain or spinal cord (Figure 4e and f; Extended Data Fig 10a). Post-immunization, *Apom*^{-/-} brains and spinal cords displayed significantly increased vascular leakage. This was dependent upon the immune response, since pertussis toxin alone was insufficient to induce vascular leakage (Extended Data Fig 10b). Thus, the BBB was intact in mice lacking ApoM before MOG₃₅₋₅₅ immunization and induction of an immune response was necessary for the generation of EAE and associated BBB breakdown.

S1P₁ ECKO mice have increased pulmonary vascular leakage (Extended data Fig 10c); however, deletion of endothelial *S1pr1* did not influence EAE disease severity (Figure 4g), suggesting that alterations in vascular barrier function are not sufficient to modulate autoimmune responses in the CNS. Similarly, S1P₁ expression by astrocytes has been shown to affect EAE severity³⁰. Since neurovascular leakage would be a necessary antecedent for plasma ApoM-S1P to gain access to astrocytes, it seems unlikely that the increased disease severity seen in *Apom*^{-/-} mice is due to direct ApoM effects on neural cells. Collectively, these data strongly suggest that ApoM-S1P signaling in lymphocytes is a key factor in the increased EAE pathology displayed by *Apom*^{-/-} mice.

In summary, these data reveal an unexpected mechanism whereby ApoM⁺HDL specifically restrains BM lymphopoiesis by inducing S1P / S1P₁ receptor signaling in BM progenitors, thereby limiting the lymphocyte compartment. These findings also suggest that unique functions of S1P are imparted by its chaperone, ApoM⁺HDL, and that ApoM⁺HDL-dependent S1P/S1P₁ signaling induces distinct physiological outcomes. While dispensable for lymphocyte trafficking, ApoM-S1P attenuation of lymphopoiesis under homeostasis may be an important regulator of the lymphocyte life cycle, and therefore have a role in autoimmune responses. Our studies indicate that ApoM⁺HDL-mediated regulation of lymphocyte ontogeny impacts the extent and intensity of autoimmune neuroinflammation in the EAE model. Furthermore, chaperone-dependent S1P signaling may afford the development of novel strategies for the control of immune responses.

Methods

Animals

Apom^{-/-} and *ApoM*^{Tg} mice were crossed at least 9 generations to the C57BL/6 genetic background^{3,31}. C57BL/6 mice purchased from Jackson Laboratory were used as wild-type controls. To generate mice that over-express S1P₁, mice expressing the *S1p1^{f/stop/f}* transgene were crossed to mice expressing the tamoxifen-inducible *Rosa26-Cre-ERT2* to yield *S1p1^{f/stop/f} Rosa26-Cre-ERT2* animals¹⁵. To generate mice with endothelial cell-specific deletion of *S1pr1*, mice with floxed *S1p1* genes (*S1pr1^{f/f}*) were crossed with mice expressing a tamoxifen-inducible Cre under the control of the VE-cadherin gene (*Cdh5-Cre-ERT2*)^{15,32}. For both *S1pr1* over-expressing mice (*S1pr1* OE) and endothelial cell-specific deletion (ECKO), Cre negative littermates were used as controls. To induce deletion of the floxed *S1p1r* or floxed “stop” sequence, mice were treated with tamoxifen by oral gavage, 4 mg every third or fifth day for a total of three treatments. *S1pr1* OE mice were analyzed 3-4 days after the final tamoxifen administration; ECKO mice were analyzed 10 days after the final tamoxifen administration. S1P₁ GFP signaling mice were generated as previously described⁴. Briefly, mice expressing a transcriptional unit consisting of the S1P₁ C-terminus fused to tTA (tetracycline transcriptional activator) and β-arrestin fused to TEV (tobacco etch virus) protease knocked in to the endogenous S1P₁ locus were crossed with mice containing a histone-GFP reporter gene under the control of a tTA-responsive promoter. Mice expressing one allele of both the *S1pr1Ki* and the GFP alleles were considered S1P₁ GFP signaling mice. Littermates expressing only the GFP allele without the S1P₁ knock-in were considered controls. For all bone marrow studies, animals were sacrificed and tissues

collected between 12 P.M. and 3 P.M to limit circadian effects. No randomization method was used and investigators were blinded to the genotype of animals during data analysis. The minimum number of animals per group was four and for all inducible Cre strains wild-type littermate controls were used. Male and female mice were used as age-matched controls for all studies except for EAE experiments, where only female animals were used. No animals were excluded from the analysis. Animals were housed in a specific pathogen-free facility and provided food and water *ad libitum*. All animal protocols were approved by the IACUC of Weill Cornell Medical College.

Verification of S1P₁ mRNA over-expression and floxed “stop” excision

After completion of the tamoxifen treatment regimen, RNA was extracted from whole bone marrow with Trizol according to the manufacturer's instructions, and TaqMan real-time multiplex RT-PCR performed as described below to assess over-expression of *S1pr1* mRNA. For extraction of genomic DNA from the same samples, back extraction buffer (1M Tris, pH 8.0, 4M guanidine thiocyanate, 50mM sodium citrate) was added to the remaining organic and interphases, vortexed, and incubated for 10 minutes at room temperature. Samples were then centrifuged at 4°C for 15 minutes at 12,000 × g and the aqueous phase transferred to a new tube. DNA was precipitated with 400 µl isopropanol and samples centrifuged again at 4°C for 15 minutes at 12,000 × g. Supernatant was removed, samples washed with 75% ethanol and the DNA pellet was resuspended in H₂O. PCR was performed using 20 ng of DNA, the following primers: 5': gtt cgg ctt ctg gcg tgt ga; 3': cca ggt cct cct cgg aga tc; and the reaction conditions: 95°C/30", 56°C/30", 72°C/1" for 30 cycles. Amplification of the intact floxed *stop* cassette yielded a 1.4 bp fragment and when deleted, a 308 bp fragment.

Blood and lymph: cell and plasma collection

Mice were euthanized with CO₂. Blood was recovered via terminal cardiac puncture and collected in tubes containing 35 µl 0.1M EDTA. 500 µl of whole blood was then removed to a new tube, centrifuged at 2,000 × g for 15 minutes, and plasma removed and stored at -20°C. Cells were then subjected to ammonium chloride (ACK) erythrocytelysis, washed with PBS, and stained with eFluor718 fixable viability dye (eBioscience) according to manufacturer's instructions. Lymph was recovered from the cisterna chyli, as previously described^{2,33}, and collected in 5 µl acid citrate-dextrose. Total lymph volume was recorded before the entire sample was centrifuged at 2,000 × g for 15 minutes to isolate plasma. Plasma was then removed and cells were washed with PBS before staining with the eFluor718 viability dye. After a PBS wash, blood and lymph cells were then briefly fixed for 30 minutes in 0.1% paraformaldehyde (PFA), washed, and stained with antibody cocktails for flow cytometry, as described below³⁴.

Tissue cell isolation

Single-cell suspensions were created from spleen, thymus, and lymph nodes (two inguinal and brachial lymph nodes per mouse) by gently disaggregating tissue between frosted glass slides. Bone marrow cells were collected after removing the epiphyses and a brief centrifugation in a 1.5mL tube. Cells were then washed with 1% FBS in PBS and subjected

to ACK lysis buffer. After another PBS wash, cells were stained with eFluor718 viability dye. For some studies, such as cell sorting, cells were stained for and analyzed by flow cytometry unfixed. For except for studies requiring live sorted cells, samples were gently fixed with 0.1% PFA for 10 minutes then washed with 1% FBS in PBS, unless noted otherwise. Although absolute numbers were lower after fixation, this did not have a dramatic effect on staining patterns and gave results similar to those obtained using unfixed cells.

Flow cytometry

After fixation, cells were washed with 1% FBS in PBS (flow buffer; FB) and Fc receptors blocked with TruStain FcX (Biolegend) in 3% FBS overnight at 4°C. Cells were then aliquoted and stained in their respective antibody cocktails for 30 minutes on ice. After washing with FB, liquid counting beads (BD) were added to each sample and data were obtained on a BD LSRII (Becton Dickson) and analyzed using FlowJo software (Tree Star, Inc.).

Antibodies were purchased from BioLegend (BL), eBioscience (eB), Southern Biotech (SB), or Becton Dickson (BD). For the determination of blood and lymph cell populations the following clones and antibody-fluorophore conjugates were used: CD4-PE (RM4-4, BL), CD8-PerCP/eFluor710 (H35-17.2; eB), CD19-eFluor450 (ID3; eB), CD11b-APC-eFluor780 (M1/70; eB), Ly6C-FITC (HK1.4; SB), Ly6G-PE-Cy7 (1A8; BL), and CD115-APC (AFS98; BL). For determination of lymph node and splenocyte populations: CD4-APC-Cy7 (GK1.5; BL), CD8-eFluor450 (H35-17.2; eB), B220-AF700 (RA3-6B2; eB), CD62L-PerCP-Cy5.5 (MEL-14; BL), and CD69- PE-Cy7 (H1.2F3; eB). *For determination of thymocyte populations:* CD3-APC-Cy7 or -AF700 (17A2; eB), CD4-PE (RM4-4, BL), CD8-APC (53-6.7, eB), CD62L- PerCP-Cy5.5 (MEL-14; BL), CD69- PE-Cy7 (H1.2F3; eB), CD44-AF700 or -PECy7 (IM7; eB), CD25-AF488 (3C7; eB), cKit-PerCP-eFluor710 or -APC-eFluor780 (CD117; 2B8; eB). DN1 (ETP) were defined as CD4⁻ CD8⁻ CD3⁻ CD44⁺ CD25⁻ cKit⁺; DN2 were defined as CD4⁻ CD8⁻ CD3⁻ CD44⁺ CD25⁺; DN3 were defined as CD4⁻ CD8⁻ CD3⁻ CD44^{lo/-} CD25⁺; DN4 were defined as CD4⁻ CD8⁻ CD3⁻ CD44⁻ CD25⁻. *For determination of bone marrow B cell populations:* B220-AF700, cKit-APC-eFluor780, CD19-PE-Cy7, Flt3-PE, CD24-BV421, CD43-AF488, IgM-PerCP-Cy5.5, IgD-APC. Pro-B cells were defined as B220⁺ cKit⁺ CD19⁺ Flt3⁻ CD24⁺ IgM⁻; pre-B cells were defined as B220⁺ cKit⁻ CD19⁺ Flt3⁻ CD24⁺ IgM⁻; immature B cells were defined as B220⁺ cKit⁻ CD19⁺ Flt3⁻ CD24⁺ IgM⁺; and mature B cells were defined as B220⁺ cKit⁻ CD19⁺ Flt3⁻ CD24^{lo/-} IgM^{+/-} IgD⁺. To quantify bone marrow cell populations with or without BrdU^{18-20,35-37}: Lineage (Lin) cocktail-eFluor450 (17A2, RA3-6B2, M1/70, Ter-119, RB6-8C5; eB), Flt3-PE (CD135; A2F10; eB), cKit-PerCP-eFluor710 or -APC-eFluor780 (CD117; 2B8; eB), Sca-1-PE-Cy7 (Ly6A/E; D7; eB), IL-7R α -APC-eFluor780, -FITC, or BV421 (CD127; A7R34; eB or SB/199; BD), CD34-APC (RAM34; BD), Fc γ RII/III-AF700 (93; eB), BrdU-PerCP-eFluor710 (BU20A; eB). For low abundance markers (cKit, Sca1, IL-7R α , CD34, Fc γ RII/III, CD25, or CD44), fluorescence minus one (FMO) controls were used to set staining gates.

For S1P₁ staining, tibiae bone marrow were spun into a tube containing 35 μ l EDTA, then immediately fixed with 0.1% PFA on ice for 1 hour. After washing with 100nM HEPES in

PBS, nonspecific interactions were blocked with anti-CD16/32 at room temperature for 15 minutes. Cells were then aliquoted for anti-S1P₁ or isotype staining (R & D) overnight at 4°C. The next day, cells were washed twice with PBS-HEPES and stained to identify bone marrow populations.

Phosphoflow for phospho-Stat5 and phospho-Erk1/2

Whole bone marrow cells were resuspended in Lyse/Fix buffer (BD Biosciences) and processed according to manufacturer's instructions. To permeabilize, 100% methanol pre-cooled at -80° was added and cells vortexed for 15 seconds before 45 minute incubation on ice. After washing with 3% FBS in PBS, cells were incubated in Fc block (anti-CD16/32) and Innovex Biosciences peptide Fc block at room temperature for 20 minutes before incubation with antibody cocktails. For detection of phospho epitopes in CLP, the following antibodies were used: Lineage cocktail-PE, cKit-PerCP-eFluor 710, Sca1-PE-Cy7, and CD127-BV421. Anti-p-Stat5 (pY694) and p-Erk1/2 (pT202/pY204) were conjugated to AF488. As controls, splenocytes were isolated from WT mice and incubated with IL-7 (10 ng/mL; pSTAT5) or PMA (5 ng/mL; pERK1/2) or left unstimulated. After 15 minutes, Lyse/Fix buffer with 30% FBS was immediately added to cells to preserve the phosphor epitopes. Cells were then processed as described above for BM samples. CD11b⁺ cells were considered the negative control for pSTAT5 in response to IL-7 stimulation. CD19⁺ cells were considered the positive controls for pSTAT5 and pERK1/2^{34,38}.

Drug administration

FTY720 (fingolimod/Gilenya™) was administered p.o. at a single dosage of 0.5 mg/kg in 200 µl of 2% 2-hydroxypropyl-β-cyclodextran (HβC; Sigma-Aldrich). AUY954 was dissolved in DMSO and administered p.o. at a single dosage of 3 mg/kg in 200 µl of 2% HβC. Both FTY720 and AUY954 were kind gifts from Novartis Pharma, AG (Basel, Switzerland). SEW2871 (Cayman Chemical, Ann Arbor, MI) was dissolved in 1:4 Tween-20 and ethanol, then administered twice at 0h and 12h at a dosage of 20 mg/kg p.o. in 200 µl of HβC before sacrifice at 24h. For all studies, control animals were treated with the appropriate vehicle.

Albumin ELISA

Albumin concentrations in blood and lymph plasmas were determined using the mouse albumin ELISA kit from Bethyl Labs, according to manufacturer's instructions. Blood plasma was diluted 1:1.6 × 10⁶ and lymph plasma 1:8 × 10⁵ prior to analyses.

ApoM and ApoA1 immunoblots

1 µl of mouse blood plasma was first diluted in 10 µl PBS, then diluted serially 1:1 in PBS, and 1 µl of diluted lymph plasma was further diluted in 10 µl PBS. Samples were then denatured by boiling in SDS sample buffer and separated on a 12% denaturing gel. After transfer to PVDF membrane, blots were incubated overnight at 4°C with 1:1000 dilution of antibodies against ApoM (rabbit anti-human; Genetex) or ApoA1 (goat anti-mouse; AbCam) in 5% milk in Tween-20 tris-buffered saline (TBS-T). Secondary antibodies were incubated at 1:10,000 dilution in 1% TBS-T for one hour at room temperature. For

approximation of ApoM concentrations, bands for the blood plasma dilution were analyzed by densitometry using ImageJ software (NIH) to create a standard curve. Undiluted blood plasma ApoM concentrations were assumed to be approximately 900 nM. Densitometric values obtained for ApoM bands from lymph plasma were compared to the standard curve and an approximate concentration calculated, which was then normalized to lymph volume. ApoA1 was used as an internal control.

Sphingosine 1-phosphate (S1P) quantitation

Bioactive sphingolipids were extracted from blood, lymph, or HDL preparations by a single phase ethyl acetate:isopropanol:water process and quantitated by electrospray ionization-tandem mass spectrometry (ESI-MS/MS) as described previously³⁹.

Integrin blockade

Mice were injected intraperitoneally with 100 µg of anti-integrin α4 (BD Pharmingen, clone M17/4) and 100 µg of anti-integrin αL (Millipore, clone PS/2)⁴⁰ in a total of 200 µl. Fourteen hours later, mice were sacrificed and brachial and inguinal lymph nodes collected. A single cell suspension was then analyzed by flow cytometry.

Administration and quantitation of 5'-Bromo-2'-deoxyuridine (BrdU)

BrdU was solubilized in 10 mM NaOH / H₂O. 4 mg BrdU (Sigma) in 200 µl PBS was injected intraperitoneally into each mouse 2.5-3 hours before sacrifice^{37,41,42}. Control mice were injected with 200 µl of PBS alone. For quantitation of BrdU incorporation, after isolation and RBC lysis, cell suspensions were fixed in 4% paraformaldehyde (BD) at room temperature for 10 minutes, then washed in 5% FBS followed by PBS. Cells were permeabilized in 100 µl of 0.125% Dawn dishwashing detergent (Procter and Gamble) in 1x PBS for 15 minutes at room temperature, then washed twice with 1% FBS in PBS. Cells were resuspended in DNase buffer (10% FBS in 1 mM CaCl₂ and 0.1 mM MgCl₂) containing 150U of DNase per sample and incubated at 37°C for 45 minutes before washing twice in PBS. Samples were then resuspended in Fc blocking buffer and incubated with antibody cocktail for analysis by flow cytometry.

Cell cycle analysis using Hoechst 33342 DNA incorporation

Freshly isolated cells were stained with antibody cocktail (anti-Lineage, -cKit, and -Sca1), washed, then resuspended in 10 µg/mL Hoechst 33342 (Life Technologies) in 1x PBS and incubated at room temperature for 45 minutes before fixation with 0.1% PFA and flow cytometric analysis.

Bone marrow IL-7 quantitation

Complete bone marrow (BM) was collected in 5µl 0.1M EDTA, then gently triturated in 200 µl PBS. Cell suspensions were then centrifuged at 2000g for 5 minutes at 4°C, then supernatants were removed to a new tube and stored at -80°C until analysis. IL-7 expression was quantified by ELISA according to manufacturer's instructions (R & D).

Multiplex quantitative real-time RT-PCR

B cells were isolated from whole spleen single cell suspensions using the EasySep mouse CD19 positive selection kit (StemCell Technologies), followed by the EasySep mouse T cell isolation kit for negative selection of T cells. Bone marrow from WT mice was subjected to negative selection for Lin⁻ cells, then LSK (Lin⁻ cKit⁺ Sca1⁺) and CLP (Lin Kit^{lo} Sca1^{lo} IL-7R α ⁺ Flt3⁺) were collected by FACS. RNA was isolated using Trizol and concentrated using the RNA Clean and Concentrator kit (Zymo Research). Real-time RT and TaqMan PCR were performed using the TaqMan RNA-to C_T 1-step kit (Life Technologies), and primers specific for mouse *S1pr1*. Reactions were normalized to expression of the housekeeping gene *Nidogen* within the same tube using the 2^{-C_t} method⁴³ and data are represented as fold change compared to expression by splenic B cells.

Ex vivo ApoM staining of BM cells

Bone marrow was spun into a tube containing 35 μ l EDTA and the femurs flushed with, and resuspended. Cells were fixed with 0.1% paraformaldehyde at room temperature for 30 minutes and washed with PBS. Non-specific interactions were first blocked by incubation with Innovex Biosciences peptide Fc block at room temperature for 15 minutes, then 10% fatty-acid-free bovine serum albumin, Fraction V (FAF-BSA), 5% milk, and anti-CD16/32 were added to 1 mL for an additional 10 minutes. This was used in place of the suggested separation medium when cells were processed for lineage negative depletion, followed by Sca1 positive selection (both kits from Stemcell Technologies). Cells were then washed twice with BSA/milk by gentle mixing, then returning them to the magnet and pouring off liquid. Two drops of peptide Fc block with anti-CD16/32 were added to each tube and incubated at room temperature for five minutes. An aliquot of cells was set aside for staining with secondary antibody alone; the remainder was incubated with 1:200 dilution of rabbit anti-ApoM (GeneTex #62234) for 30 minutes at room temperature. Cells were washed on the magnetic column three times with BSA/milk before incubation with a 1:5000 dilution of donkey anti-rabbit AF546 (Life Technologies) for 30 minutes at room temperature. After washing again on the magnetic column, cells were incubated in PBS containing DAPI before imaging with an Olympus Fluoview Fv10i confocal microscope using the 60x water objective. Intensities for the blue and red channel were adjusted for the *ApoM*^{-/-} cells in accordance with their spectra and, once set, the same settings were used for the WT images. Thus, channel intensity correction was the same for each sample and no gamma correction was used.

Ex vivo IL-7R α staining of BM cells from S1P₁ GFP signaling mice

Bone marrow was spun into a tube containing 35 μ l EDTA and the femurs flushed with, and resuspended in, 0.1% paraformaldehyde. Cells were fixed at room temperature for 12 minutes and washed with 1% FBS in PBS before being subjected to lineage depletion followed by Sca1 positive selection. Cells were then stained with either Lin cocktail or biotinylated anti-IL-7R α primary antibody (clone SB/199; BD) followed by streptavidin-AF596 secondary antibody (Jackson Immunoresearch). All cells were incubated in DAPI in PBS before imaging by confocal microscopy, as described above.

In vitro hematopoiesis and lymphopoiesis

Lineage negative (Lin^-) BM cells from WT or S5A mice were isolated using a negative selection magnetic bead kit (StemCell Technologies). In some experiments, CLPs from WT mice were sorted by FACS. 5,000 cells were then incubated in 350 μl methylcellulose medium HPP-SP1 (MC; HemoGenix) containing IL-3, IL-6, stem cell factor (SCF), thrombopoietin (TPO), Flt3L, BSA, and 5% FBS and supplemented with 10 ng/mL rmIL-7 (Peprotech). Control wells contained only this complete medium. Data from at least two duplicate wells per experimental condition were averaged. Cells from each mouse were assayed individually and not pooled. The stock solution of W146 was prepared in filtered Na_2CO_3 buffer and sonicated until dissolved, then added to MC at a final concentration of 1 μM . AUY954 was dissolved in DMSO and diluted in MC for a final concentration of 100nM and 0.001% DMSO. FTY720p was dissolved in 1x PBS and added to MC. The vehicle control for the *in vitro* agonist/antagonist studies was 0.001% DMSO. Human and mouse HDLs were isolated by ultracentrifugation of plasma from healthy donors or mice as previously described and added to MC at the concentrations indicated⁴⁴⁻⁴⁶. The content of S1P in HDL preparations was determined by HPLC and LS/MS/MS as described above⁴⁶. For S1P neutralization by anti-S1P antibody, 50 $\mu\text{g}/\text{mL}$ HDL was incubated with 25 $\mu\text{g}/\text{mL}$ of either anti-S1P antibody (Alfresa Pharma Corp, Tokyo, Japan) or mouse IgM (Bethyl Labs) at 37°C for 1 hour, then added to the MC⁴⁷. Albumin-S1P was prepared by reconstituting stock S1P (in ethanol) in 0.1% fatty acid-free BSA (FAF-BSA; Fisher), then sonicating for 20 seconds. Dilutions were then made in 0.1% FAF-BSA before adding to MC. All MC incubations of Lin^- cells were incubated for 10 days at 37°C and 5% CO_2 .

Flow cytometric analysis of in vitro incubations

For cell collection, 500 μl of PBS was added to each well, incubated for 10 minutes, then gently triturated to resuspend the cell culture/MC mixture. Resuspended cells were removed to a 1.5mL microcentrifuge tube and cells remaining in the well were collected with an additional 500 μl of PBS. Cells were then centrifuged at 700 $\times g$ for 10 minutes at 4°C, washed once with PBS, then processed for incubation with antibody cocktail and flow cytometric analysis as described above.

Induction of EAE

EAE was induced by subcutaneous injection on both flanks and base of the tail of 200 μg myelin oligoglycoprotein (MOG₃₅₋₅₅) peptide (Alpha Diagnostic Intl. Inc.) emulsified in 200 μl of complete Freund's adjuvant (Difco). 200 ng of *Bordetella pertussis* toxin (List Biological Laboratories, Inc.) was injected intraperitoneally in 200 μl on the day of immunization and 48 hours later^{5,13}. Clinical scores were determined based on the following scale: 0, normal; 1, tail weakness; 2, tail paralysis and hind limb weakness; 3, complete hind limb paralysis; 4, hind limb paralysis with forelimb weakness and 5, moribund or death¹³. For histopathological analysis of brain tissue sections, brains were removed and fixed in 10% neutral-buffered formalin overnight at room temperature. After washing in PBS, brains were placed in 70% ethanol before paraffin embedding. Tissue sections were then stained with hematoxylin and eosin (Histoserve, Inc.).

Isolation of CNS-infiltrating immune cells

Brains from WT and *Apom*^{-/-} mice were minced, then digested in a mixing incubator for one hour at 37°C and 1300 rpm in a cocktail of Liberase (1U/1ml; Roche) and DNase (1 mg/ml; Sigma) in Hank's balanced salt solution (HBSS). Tissues were further disaggregated by repeated passage through an 18G needle, then brought to 1 ml with HBSS. Leukocytes were isolated on a discontinuous Percoll gradient according to Pino and Cardona⁴⁸ and analyzed by flow cytometry.

In vitro lymphocyte restimulation

Spleens from WT or *Apom*^{-/-} mice were isolated 9 days post-MOG₃₅₋₅₅ peptide immunization. After disaggregation and erythrocyte lysis with ammonium chloride, cells were cultured in 96-well plates at a density of 5×10^5 cells with increasing concentrations of MOG₃₅₋₅₅ peptide. After 96 hours of incubation, numbers of CD4⁺ cells were quantified by flow cytometry¹³.

Evans Blue dye extravasation measure of vascular permeability

Pulmonary vascular leakage was measured by Evans Blue dye (EBD) accumulation assay. EBD (0.5% in PBS) was injected via tail vein 90 minutes before tissue harvest. Pulmonary vasculature was perfused with 5 mL PBS through the right ventricle, while allowing the perfusate to drain from an incision in the left ventricle. Lungs were then weighed and dried at 56°C overnight. Dry lung weight was measured again, and EBD was dissolved in formamide at 37°C for 24 hours and quantitated spectrophotometrically at 620 and 740 nm.

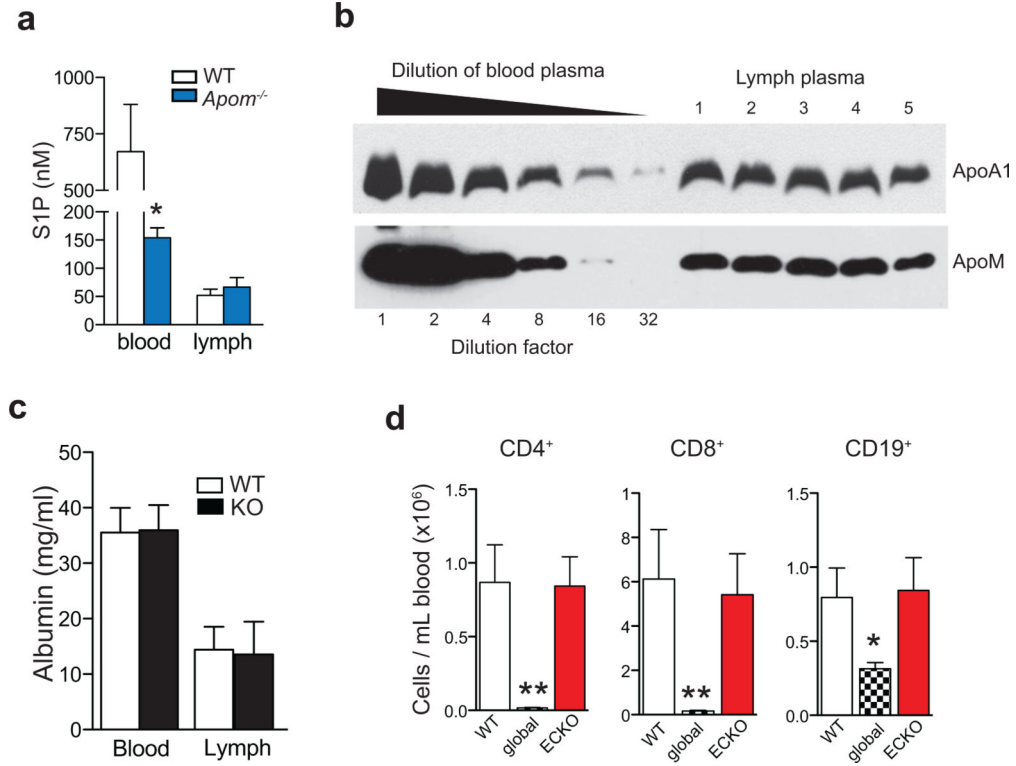
Tetramethylrhodamine (TMR) dextran brain and spinal cord vascular permeability

Eight days post-MOG immunization, MOG-immunized mice, mice injected with pertussis toxin alone, or unimmunized mice were injected via tail vein with 100 µl of 25 mg/mL TMR-dextran in 1 mM CaCl₂. After 18h, mice were sacrificed by CO₂ and perfused with approx. 10 mL PBS. Brain and spinal cord were removed and protected from light from this point. After weighing, tissues were homogenized in 1% Triton X-100 in PBS then spun at 4°C for 25 minutes at 20,000 × g. Supernatants were transferred to new tubes until fluorometric analysis at 540/590.

Statistical analyses

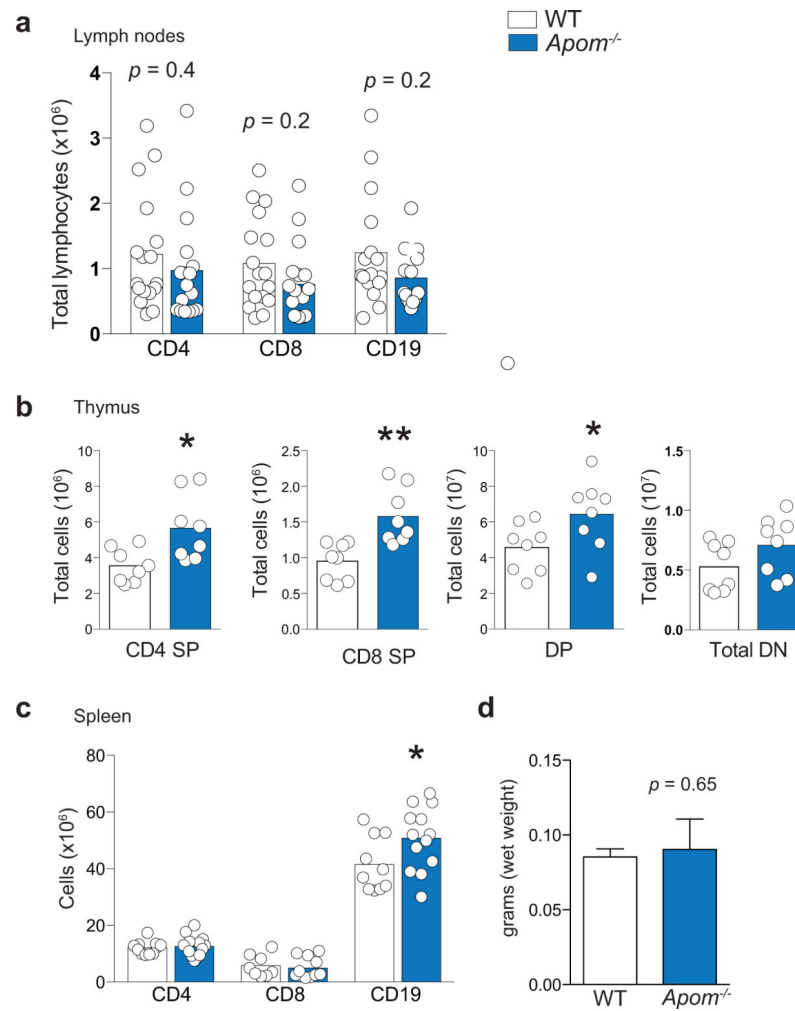
Statistical analyses were performed using GraphPad Prism software v6.0. Two-tailed Student's *t*-test was used for direct comparison of two groups. Analysis of variance (ANOVA) followed by Dunnett's for comparison to control group or Tukey's to compare all groups was used to determine significance between three or more test groups. Differences in EAE clinical scores were determined using the Mann-Whitney *U*-test for analysis of the area under the curve and at individual time points. For all analyses, α was set to 0.05 and *p* values ≤ 0.05 were considered significantly different.

Extended Data



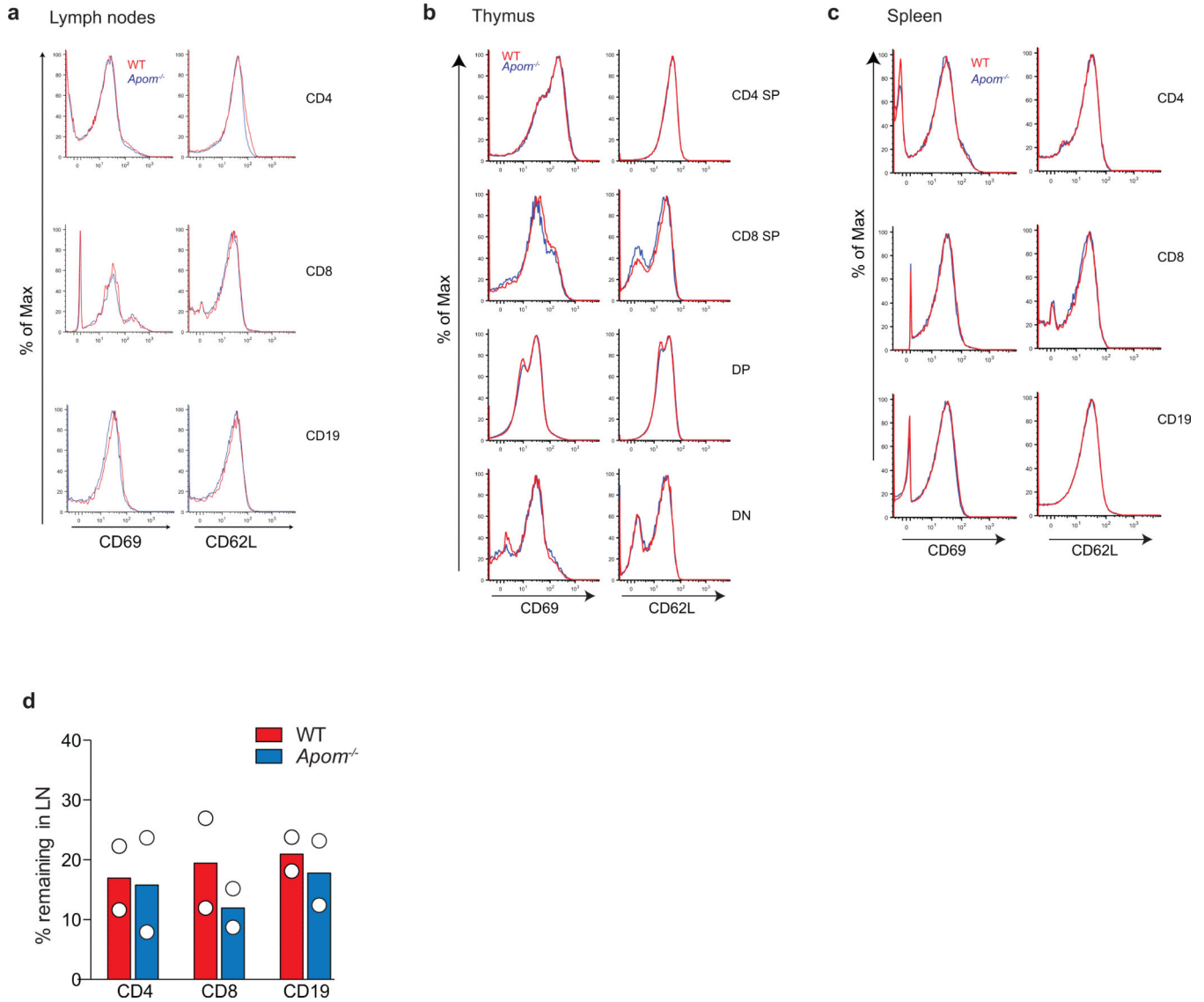
Extended Data Fig 1. Blood and lymph ApoM and albumin in WT and *Apom*^{-/-} mice and blood cell numbers in *S1pr1* global and ECKO mice

a, Concentrations of blood and lymph sphingosine 1-phosphate (S1P) were determined by LC-MS/MS. Bars represent means ± SD. *n* = 4 as described in Materials and Methods. **b**, Western blots of ApoA1 and ApoM in lymph of WT mice. 1 μl of WT blood plasma was serially diluted 1:1, and 1 μl of diluted lymph plasma from 5 animals was analyzed for ApoA1 and ApoM protein levels. **c**, Determination by ELISA of albumin concentrations in the blood and lymph of WT or *ApoM*^{-/-} (KO) mice. Bars are mean ± SD. WT, *n* = 5; *ApoM*^{-/-}, *n* = 7 **d**, Quantification of CD4, CD8, and CD19 cells in the blood of wild-type (WT), *S1pr1*^{fl/fl} *Rosa26-Cre-ER*^{T2} (global) or *S1pr1*^{fl/fl} *Cdh5-Cre-ER*^{T2} (ECKO) mice. Bars are mean ± SD. WT, *n* = 5; global or ECKO, *n* = 6. **p* < 0.05; ***p* < 0.005, as compared to WT values.



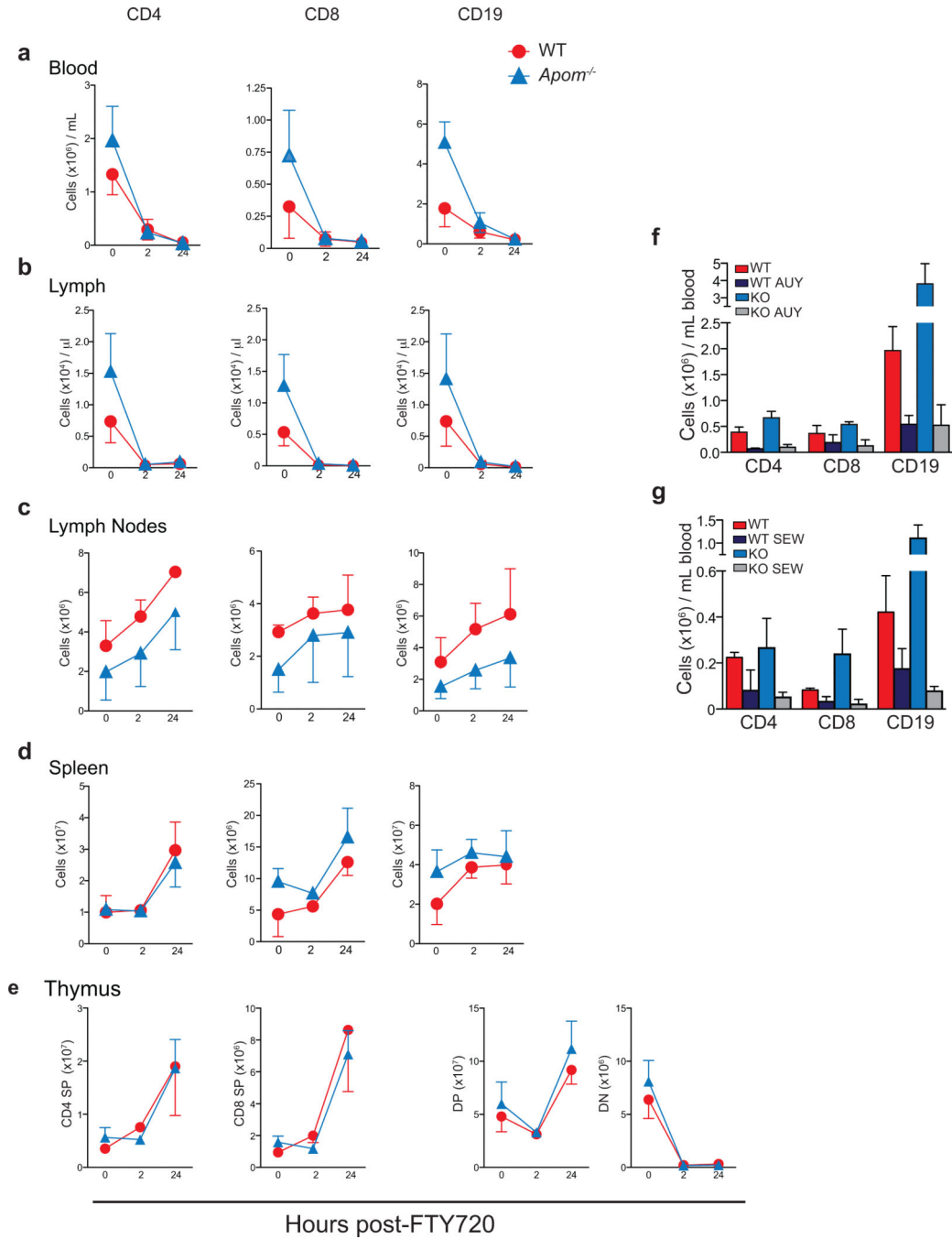
Extended Data Fig 2. Cell populations of the lymph node, thymus, and spleen are largely similar in $Apom^{-/-}$ and WT mice

a, Quantification of CD4, CD8, and CD19 cells in two brachial and two inguinal lymph nodes combined. Data are compiled from five experiments. **b**, Quantitation of CD4 single positive (SP), CD8 SP, CD4⁺CD8⁺ double positive (DP), and total CD4⁻CD8⁻ double negative (DN) cells in thymi of WT or $Apom^{-/-}$ mice. Data are compiled from three experiments. **c**, Quantitation of CD4, CD8, and CD19 cells in spleens of WT or $Apom^{-/-}$ mice. Data are compiled from three experiments. (**a-c**) Bars represent means and circles represent values obtained from individual mice. $*p < 0.05$. **d**, Total spleen weights (grams of wet weight) from WT or $Apom^{-/-}$ mice. $n = 6$. Bars represent means \pm SD.



Extended Data Fig 3. Surface expression of the maturation markers CD62L and CD69 and lymph node egress are unchanged in *Apom*^{-/-} mice

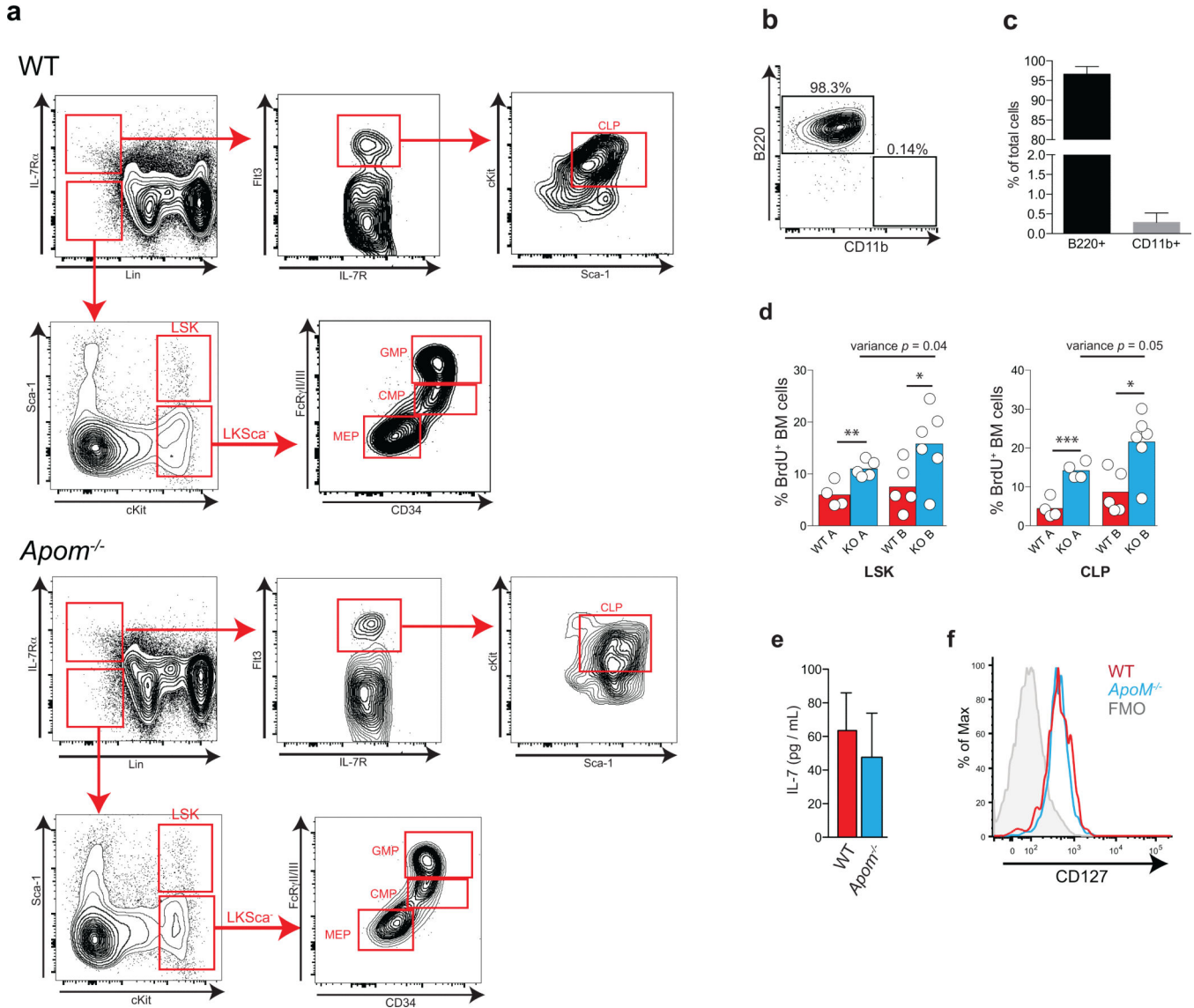
Surface expression of the lymphocyte maturation markers CD62L and CD69 was determined by flow cytometry and representative histograms are shown of staining by **a**, lymph node cells, **b**, thymocytes, or **c**, splenocytes quantified in Supplemental Fig 3 from WT (red) and *Apom*^{-/-} (blue) mice. **d**, Percent of CD4⁺, CD8⁺, and CD19⁺ cells remaining in brachial and inguinal lymph nodes 14 hours after administration of α4 and αL integrin-blocking antibodies. Symbols represent mean value acquired from three mice in independent experiments; bars represent means.



Extended Data Fig 4. ApoM expression is not required for the lymphopenia response to treatment with FTY720 or the S1P₁-specific agonists AUY954 and SEW 2871

WT (red) and *Apom*^{-/-} (blue) mice were treated with a single dose of FTY720 (0.5 mg/kg p.o.), and samples collected at 0, 2, or 24 hours post-treatment. CD4, CD8, and CD19 cells from **a**, blood, **b**, lymph, **c**, lymph node, and **d**, spleen, and CD4 SP, CD8 SP, CD4⁺CD8⁺ DP, and CD4⁻CD8⁻ DN from thymus (**e**) were quantitated by flow cytometry. Symbols represent means \pm SD and graphs are of data compiled from two experiments. 0 hours, *n* = 5; 2 hours, *n* = 6 24 hours, *n* = 4 **f**, WT and *Apom*^{-/-} mice were treated with AUY954

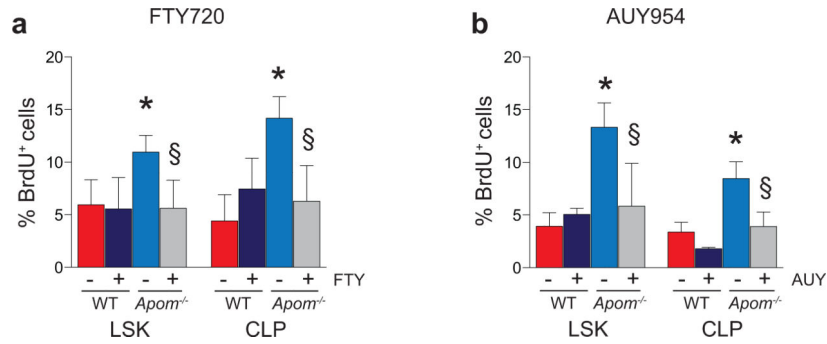
(AUY; 1 mg/kg), g, SEW2871 (SEW; 20 mg/kg), or respective vehicle controls. 24 hours post-treatment, CD4, CD8, and CD19 cells in the blood were quantitated by flow cytometry. Bars represent means \pm SD. $n = 4$ for all treatment groups and data are representative of two experiments.



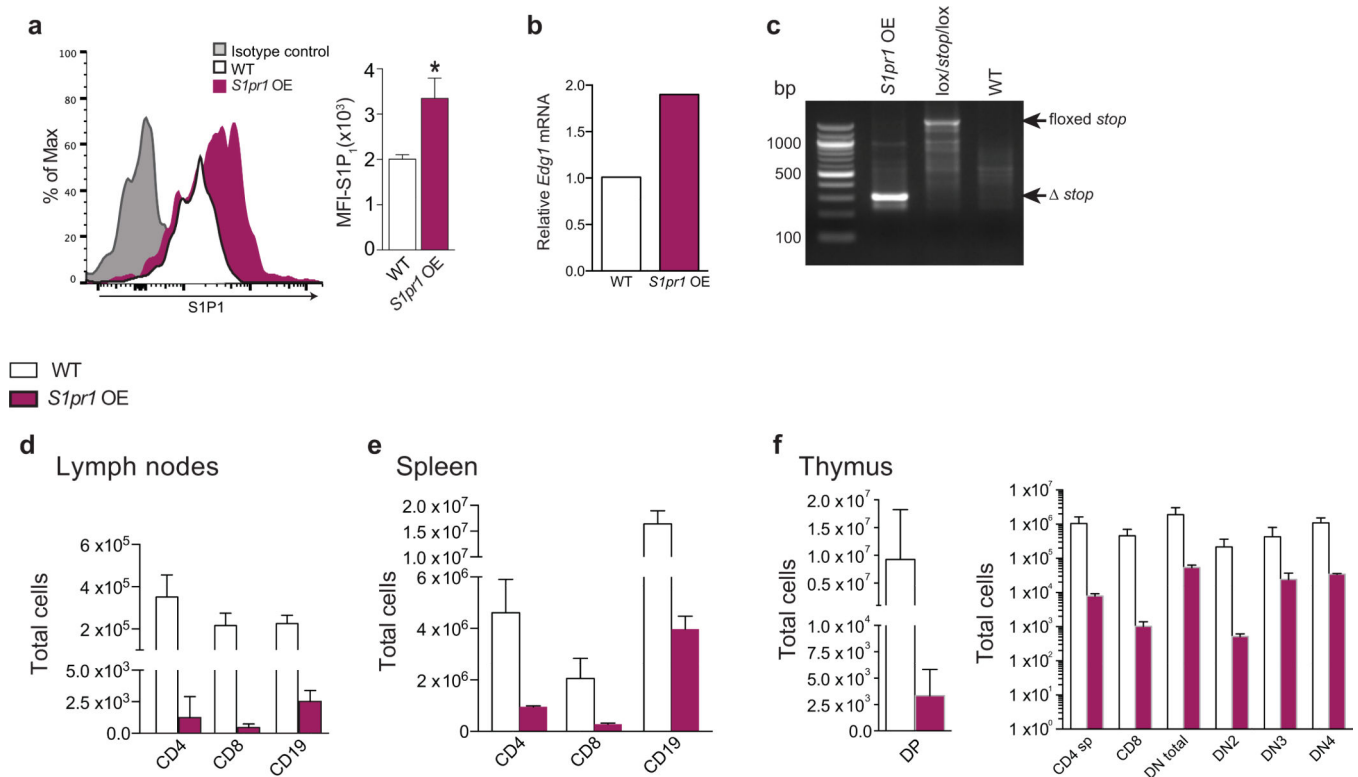
Extended Data Fig 5. Multiparameter flow cytometry gating scheme for determination of CLP and other bone marrow populations

a, Cells are first gated as Lineage (Lin⁻) and IL-7R α ⁺. Cells are then gated by Fli3 (Fik2/CD135) versus IL-7R α expression, then further gated by cKit versus Sca1 expression to define common lymphoid progenitors (CLP). Representative staining examples of WT (top) or *Apom*^{-/-} (bottom) BM cells are shown. **b**, Representative flow cytometric plot and **c**, quantitation of B220⁺CD11b⁻ and CD11b⁺B220⁻ cells generated from CLP in vitro. CLP, gated according to the gating hierarchy shown in (a), were sorted from BM of WT mice and incubated in methylcellulose medium containing growth factors to support both lymphoid

and myeloid lineage development. Cells were analyzed for B220 and CD11b expression after 12d of culture. $n = 6$. **d**, Percent BrdU incorporation by LSK (left) or CLP (right) in BM of WT (red) or *Apom*^{-/-} (blue) mice in two independent experiments (A and B). * $p < 0.05$ versus WT; ** $p = 0.006$ versus WT; *** $p = 0.0009$ versus WT. Equality of variance was determined by an *F* test. Bars represent means and circles represent values obtained from individual mice. **e**, IL-7 protein in bone marrow supernatants from WT and *Apom*^{-/-} mice were quantified by ELISA. $n = 6$ combined from two studies. Bars represent mean \pm SD. **f**, Representative histogram of IL-7R α (CD127) expression on the surface of WT (red) or *Apom*^{-/-} (blue) CLP. The fluorescence minus one (FMO) control is represented by the grey filled histogram.



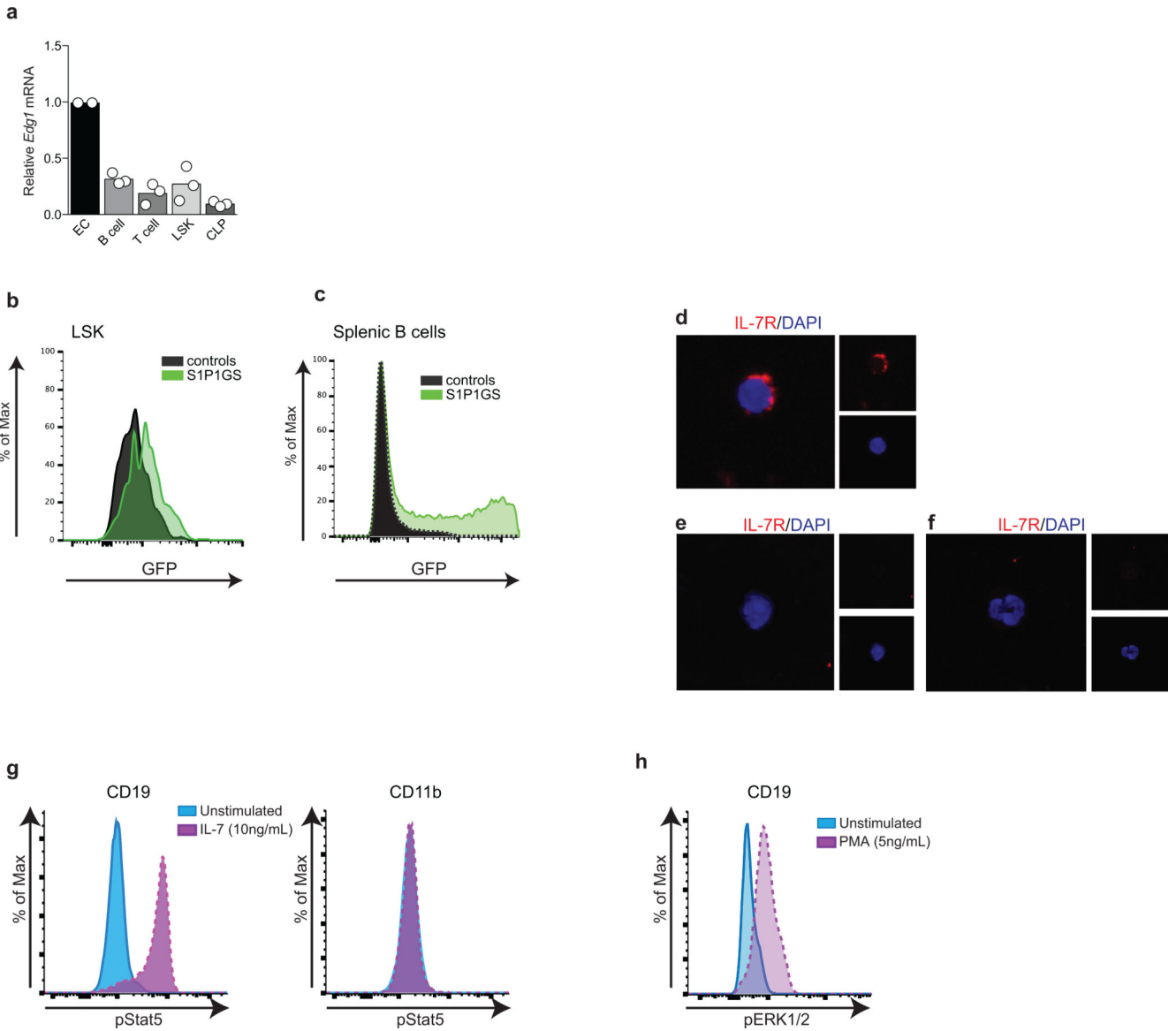
Extended Data Fig 6. Treatment with the S1P₁ modulator FTY720 or the S1P₁- specific agonist AUY954 suppresses BrdU incorporation by LSK and CLP in *Apom*^{-/-} bone marrow
 Percent BrdU incorporation 24 hours post-treatment with (a) 0.5 mg/kg FTY720 or (b) 1.0 mg/kg AUY954. (a) WT, $n = 4$; *Apom*^{-/-}, $n = 5$ for vehicle-treated and WT, $n = 7$; *Apom*^{-/-}, $n = 8$ for FTY720-treated groups. (b) Vehicle-treated, $n = 3$; AUY954-treated, $n = 6$. Bars represent means \pm SD and data are compiled from two experiments. * $p < 0.05$ versus WT; § $p < 0.05$ versus vehicle-treated control.



Extended Data Fig 7. Over-expression of S1P₁ results in marked decreases in lymphocyte populations in the thymus and secondary lymphoid organs

a, Representative flow cytometry plots and quantitative MFI of S1P₁ expression by Lin⁻ cells from *S1pr1* OE and WT littermates. *n* = 3. **b**, Relative expression levels of *S1pr1* mRNA in bone marrow cells of *S1pr1* OE mice relative to WT mice, as determined by multiplex qRT-PCR. **c**, Representative agarose gel of Cre activation and excision of the floxed *Stop* cassette as assessed by PCR of genomic DNA from bone marrow cells of *S1pr1* OE, *lox/stop/lox* littermate, or WT littermate. Arrows indicate amplified DNA fragments corresponding to undeleted or deleted segments

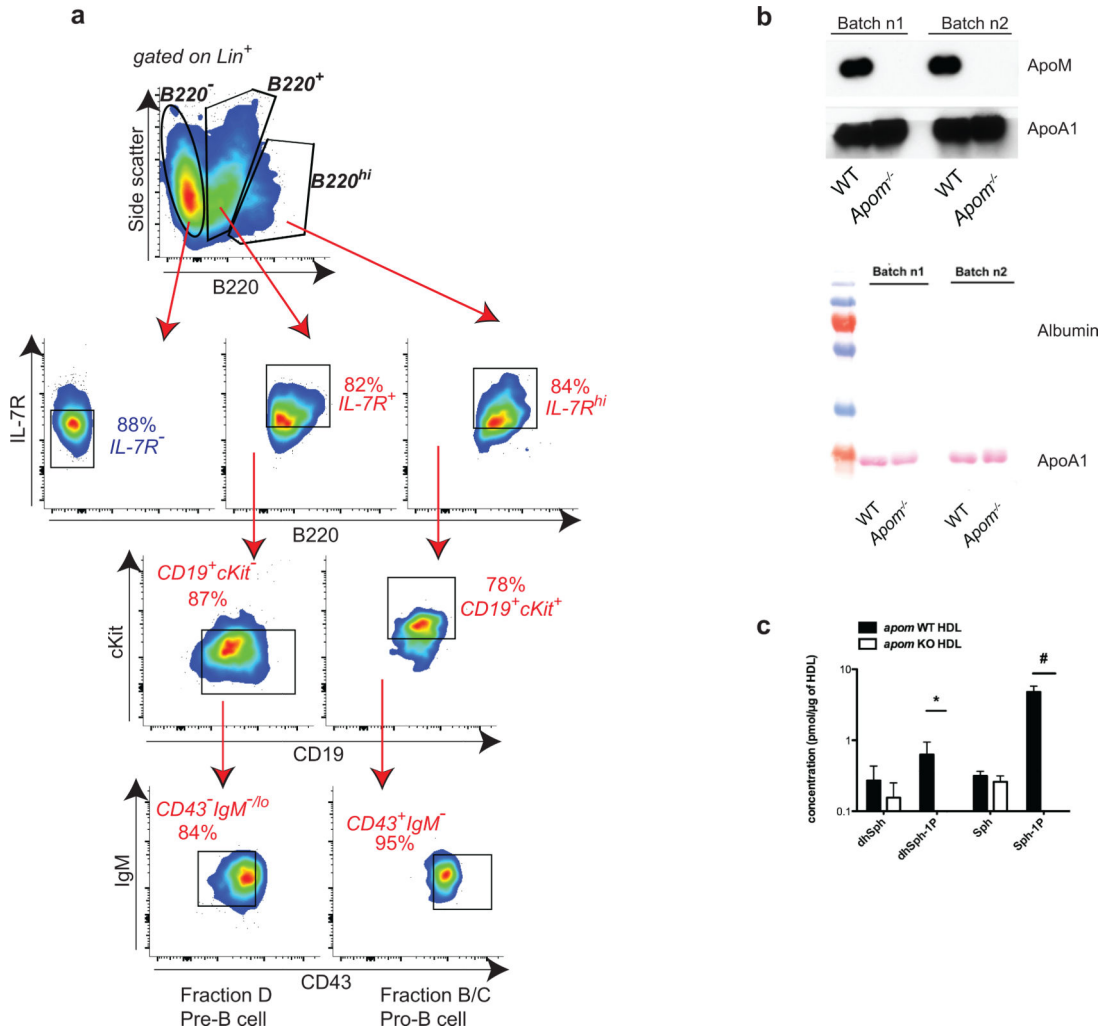
Four days after the final dose of tamoxifen, CD4⁺, CD8⁺, and CD19⁺ cells in **(d)** brachial and inguinal lymph nodes and **(e)** spleen, and **(f)** thymic CD4⁺CD8⁺ double positive (DP), CD4 and CD8 single positive (CD4 or CD8 sp), total double negative (DN), and double negative subpopulations DN2, DN3, and DN4 were quantified by flow cytometry in *S1pr1* OE mice and WT littermates. Bars represent means ± SD; *S1pr1* OE, *n* = 6; WT, *n* = 7 and data are compiled from two experiments.



Extended Data Fig 8. GFP expression by BM cells and splenocytes of S1P₁ GFP signaling mice and stimulation of STAT5 or ERK1/2 phosphorylation in splenocytes

a, Relative expression levels of *S1pr1* mRNA in LSK and CLP from bone marrow, or splenic B or T cells of WT mice relative to mouse endothelial cells, as determined by multiplex qRT-PCR. Bars represent means and circles represent values obtained from individual mice. **b**, Representative histograms of GFP expression by LSK from BM of S1P₁ GFP signaling mice (S1P1GS; green) or control (black) mice. **c**, Representative histogram of GFP expression by splenic B cells (CD19) from S1P₁ GFP signaling mice (green) or control (black) mice, demonstrating high in vivo GFP expression. **d**, Representative immunofluorescence image of IL-7R α ⁺ cell with CLP morphology from BM of littermate control of S1P₁ GFP signaling mice. Cells were subjected to the same selection process before immunofluorescence staining. IL-7R α , red; blue, DAPI, (**e and f**) Staining of BM cells from S1P₁ GFP signaling mouse littermate controls demonstrates IL-7R α staining

specificity: cells with (e) CLP morphology stained with secondary alone or (f) myeloid cell morphology from BM stained with anti-IL-7R α exhibit no IL-7R α positivity. IL-7R α , red; blue, DAPI. g, pSTAT5 staining after in vitro stimulation of WT splenocytes with IL-7 (10 ng/mL) for 15 minutes. CD19⁺ cells serve as positive controls for pSTAT5 staining. CD11b⁺ cells serve as negative controls, since they do not have IL-7R and therefore do not respond to IL-7 stimulation with STAT5 phosphorylation. h, pERK1/2 staining after in vitro stimulation of WT splenocytes with PMA (5 ng/mL) for 15 minutes. CD19⁺ cells serve as positive controls for pERK1/2 staining.

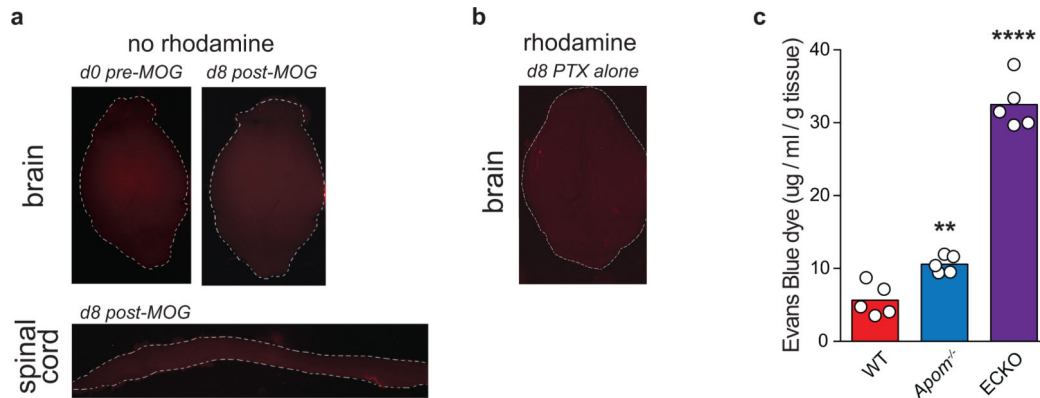


Extended Data Fig 9. In vitro lymphopoiesis in the presence of ApoM⁺HDL generates B cells at different stages of development

a, Phenotyping of B220⁺ cell populations generated from WT Lin⁻ BM after eight days of culture in methylcellulose medium. Initially, cells were gated as B220⁻, B220⁺, or B220^{hi}. From populations expressing B220, pro-B cell (Hardy fractions B/C) and pre-B cell (Hardy fraction D) equivalents were identified. Pro-B cells were defined as IL-7R^{hi}, CD19⁺, cKit⁺, CD43⁺, and IgM⁻. Pre-B cells were defined as IL-7R⁺, CD19⁺, cKit⁻, CD43⁻, and IgM^{-/lo}.

b, Western blot analysis of two batches of mouse HDL (Batches n1 and n2) isolated from

WT or *Apom*^{-/-} mice showing the absence of contaminating albumin. **c**, Liquid chromatography tandem mass spectrometric (LC-MS/MS) analysis of HDL isolated from pooled plasmas of WT or *Apom*^{-/-} mice. **p* < 0.05, #*p* < 0.005. *n* = 3. dhSph, dihydrosphingosine; dhSph-1P, dihydro-sphingosine 1-phosphate; Sph, Sphingosine; Sph-1P, Sphingosine 1-phosphate.



Extended Data Fig 10.

a, Representative photographs of auto-fluorescence in whole brains or spinal cord in WT mice at d0 or d8 post-MOG₃₅₋₅₅ immunization. *No rhodamine* denotes tissues from animals that were not injected with TMR-dextran. **b**, Representative photograph of whole brain 16h after TMR-injection of a mouse injected with pertussis toxin (PTX) alone, without accompanying MOG₃₅₋₅₅ immunization. **c**, Pulmonary vascular permeability as determined by Evans Blue dye extravasation in wild-type (WT), *Apom*^{-/-}, and S1P₁ EC-specific knockout (ECKO) mice. Bars represent means and circles represent values from individual animals. ***p* < 0.005, *****p* < 0.0001, as compared to WT controls.

Acknowledgments

The authors thank Carl Nathan, Gary Koretzky and Ralph Nachman for critical comments, Christina Christoffersen and Lars Bo Nielsen for the *Apom*^{-/-} and *Apom*^{T8} mice and discussions, Volker Brinkmann and Novartis Pharma, A.G. for the kind gifts of FTY720 and AUY954, Marie Sanson for the help with HDL purification, Yinxiang Huang for help with the EAE model and Jason McCormick for assistance with FACS. V.A.B. is a Leon Levy Research Fellow of the Weill Cornell Medical College Brain and Mind Institute. Research was supported by grants to V.A.B. (NIH F32 CA14211 and NYS C026878), T. H. (NIH HL67330, HL70694, HL89934, and Fondation LeDucq), R.L.P. (Intramural program of the NIDDK, NIH, and Fondation LeDucq), M.H. and L.S. (Fondation LeDucq) the Lipidomics Shared Resource, Hollings Cancer Center, Medical University of South Carolina (P30 CA138313) and the Lipidomics Core in the SC Lipidomics and Pathobiology COBRE (P20 RR017677).

References

1. Cyster JG, Schwab SR. Sphingosine-1-phosphate and lymphocyte egress from lymphoid organs. *Annu. Rev. Immunol.* 2012; 30:69–94. [PubMed: 22149932]
2. Schwab SR, et al. Lymphocyte sequestration through S1P lyase inhibition and disruption of S1P gradients. *Science.* 2005; 309:1735–1739. [PubMed: 16151014]
3. Christoffersen C, et al. Endothelium-protective sphingosine-1-phosphate provided by HDL-associated apolipoprotein M. *Proc. Natl. Acad. Sci. U.S.A.* 2011; 108
4. Kono M, et al. Sphingosine-1-phosphate receptor 1 reporter mice reveal receptor activation sites in vivo. *J. Clin. Invest.* 2014; 124:2076–2086. [PubMed: 24667638]

5. Furlan R, Cuomo C, Martino G. Animal models of multiple sclerosis. *Methods Mo.l Biol.* 2009; 549:157–173.
6. Hannun Y, Obeid L. Principles of bioactive lipid signalling: lessons from sphingolipids. *Nat. Rev. Mol. Cell Biol.* 2008; 9:139–150. [PubMed: 18216770]
7. Chun J, Hla T, Lynch KR, Spiegel S, Moolenaar WH. International Union of Basic and Clinical Pharmacology. LXXVIII. Lysophospholipid receptor nomenclature. *Pharmacol. Rev.* 2010; 62:579–587. [PubMed: 21079037]
8. Faber K, Axler O, Dahlbäck B, Nielsen LB. Characterization of apoM in normal and genetically modified mice. *J. Lipid Res.* 2004; 45:1272–1278. [PubMed: 15102887]
9. Christoffersen C, et al. Isolation and characterization of human apolipoprotein M-containing lipoproteins. *J. Lipid Res.* 2006; 47:1833–1843. [PubMed: 16682745]
10. Kimura T, et al. Sphingosine 1-phosphate may be a major component of plasma lipoproteins responsible for the cytoprotective actions in human umbilical vein endothelial cells. *J. Biol. Chem.* 2001; 276:31780–31785. [PubMed: 11427538]
11. Allende ML, Dreier JL, Mandala S, Proia RL. Expression of the sphingosine 1-phosphate receptor, S1P₁, on T-cells controls thymic emigration. *J. Biol. Chem.* 2004; 279:15396–15401. [PubMed: 14732704]
12. Brinkmann V, et al. Fingolimod (FTY720): discovery and development of an oral drug to treat multiple sclerosis. *Nat. Rev. Drug Discov.* 2010; 9:883–897. [PubMed: 21031003]
13. Garris CS, et al. Defective sphingosine 1-phosphate receptor 1 (S1P₁) phosphorylation exacerbates T_H17-mediated autoimmune neuroinflammation. *Nat. Immunol.* 2013; 14:1166–1172. [PubMed: 24076635]
14. Liu G, Yang K, Burns S, Shrestha S, Chi H. The S1P₁ mTOR axis directs the reciprocal differentiation of T_H1 and T_{reg} cells. *Nat. Immunol.* 2010
15. Jung B, et al. Flow-Regulated Endothelial S1P Receptor-1 Signaling Sustains Vascular Development. *Dev. Cell.* 2012; 23:600–610. [PubMed: 22975328]
16. Jo E, et al. S1P₁-selective in vivo-active agonists from high-throughput screening: off-the-shelf chemical probes of receptor interactions, signaling, and fate. *Chem.Biol.* 2005; 12:703–715. [PubMed: 15975516]
17. Thangada S, et al. Cell-surface residence of sphingosine 1-phosphate receptor 1 on lymphocytes determines lymphocyte egress kinetics. *J. Exp. Med.* 2010; 207:1475–1483. [PubMed: 20584883]
18. Yvan-Charvet L, et al. ATP-binding cassette transporters and HDL suppress hematopoietic stem cell proliferation. *Science.* 2010; 328:1689–1693. [PubMed: 20488992]
19. Massberg S, et al. Immunosurveillance by hematopoietic progenitor cells trafficking through blood, lymph, and peripheral tissues. *Cell.* 2007; 131:994–1008. [PubMed: 18045540]
20. Kondo M, Weissman IL, Akashi K. Identification of clonogenic common lymphoid progenitors in mouse bone marrow. *Cell.* 1997; 91:661–672. [PubMed: 9393859]
21. Beck TC, Gomes AC, Cyster JG, Pereira JP. CXCR4 and a cell-extrinsic mechanism control immature B lymphocyte egress from bone marrow. *J. Exp. Med.* 2014
22. Westerterp M, et al. Regulation of hematopoietic stem and progenitor cell mobilization by cholesterol efflux pathways. *Cell Stem Cell.* 2012; 11:195–206. [PubMed: 22862945]
23. Armstrong AJ, Gebre AK, Parks JS, Hedrick CC. ATP-binding cassette transporter G1 negatively regulates thymocyte and peripheral lymphocyte proliferation. *J. Immunol.* 2010; 184:173–183. [PubMed: 19949102]
24. Feng H, et al. Deficiency of scavenger receptor BI leads to impaired lymphocyte homeostasis and autoimmune disorders in mice. *Arterioscler. Thromb. Vasc. Biol.* 2011; 31:2543–2551. [PubMed: 21836069]
25. Mazzucchelli R, Durum SK. Interleukin-7 receptor expression: intelligent design. *Nat. Rev. Immunol.* 2007; 7:144–154. [PubMed: 17259970]
26. Clark MR, Mandal M, Ochiai K, Singh H. Orchestrating B cell lymphopoiesis through interplay of IL-7 receptor and pre-B cell receptor signalling. *Nat. Rev. Immunol.* 2014; 14:69–80. [PubMed: 24378843]

27. Oo ML, et al. Engagement of S1P1-degradative mechanisms leads to vascular leak in mice. *J. Clin. Invest.* 2011; 121:2290–2300. [PubMed: 21555855]
28. Weinstock-Guttman B, et al. Serum lipid profiles are associated with disability and MRI outcomes in multiple sclerosis. *J. Neuroinflammation.* 2011; 8:127. [PubMed: 21970791]
29. Weinstock-Guttman B, Zivadinov R, Ramanathan M. Inter-dependence of vitamin D levels with serum lipid profiles in multiple sclerosis. *J. Neurol. Sci.* 2011; 311:86–91. [PubMed: 21849177]
30. Choi JW, et al. FTY720 (fingolimod) efficacy in an animal model of multiple sclerosis requires astrocyte sphingosine 1-phosphate receptor 1 (S1P₁) modulation. *Proc. Natl. Acad. Sci. U.S.A.* 2010; 108:751–756. [PubMed: 21177428]
31. Christoffersen C, et al. Effect of apolipoprotein M on high density lipoprotein metabolism and atherosclerosis in low density lipoprotein receptor knock-out mice. *J. Biol. Chem.* 2008; 283:1839–1847. [PubMed: 18006500]
32. Pitulescu ME, Schmidt I, Benedito R, Adams RH. Inducible gene targeting in the neonatal vasculature and analysis of retinal angiogenesis in mice. *Nat. Protoc.* 2010; 5:1518–1534. [PubMed: 20725067]
33. Matloubian M, et al. Lymphocyte egress from thymus and peripheral lymphoid organs is dependent on S1P receptor 1. *Nature.* 2004; 427:355–360. [PubMed: 14737169]
34. Kalaitzidis D, Neel BG. Flow-cytometric phosphoprotein analysis reveals agonist and temporal differences in responses of murine hematopoietic stem/progenitor cells. *PloS one.* 2008; 3:e3776. doi:10.1371/journal.pone.0003776. [PubMed: 19020663]
35. Ding L, Morrison SJ. Haematopoietic stem cells and early lymphoid progenitors occupy distinct bone marrow niches. *Nature.* 2013; 495:231–235. [PubMed: 23434755]
36. Akashi K, Traver D, Miyamoto T, Weissman IL. A clonogenic common myeloid progenitor that gives rise to all myeloid lineages. *Nature.* 2000; 404:193–197. [PubMed: 10724173]
37. Passegue E, Wagers AJ, Giuriato S, Anderson WC, Weissman IL. Global analysis of proliferation and cell cycle gene expression in the regulation of hematopoietic stem and progenitor cell fates. *J. Exp. Med.* 2005; 202:1599–1611. [PubMed: 16330818]
38. Krutzik PO, Clutter MR, Nolan GP. Coordinate analysis of murine immune cell surface markers and intracellular phosphoproteins by flow cytometry. *J. Immunol.* 2005; 175:2357–2365. [PubMed: 16081806]
39. Bielawski J, et al. Comprehensive quantitative analysis of bioactive sphingolipids by high-performance liquid chromatography-tandem mass spectrometry. *Meth. Mol. Biol.* 2009; 579:443–467.
40. Pham THM, Okada T, Matloubian M, Lo CG, Cyster JG. S1P1 receptor signaling overrides retention mediated by G alpha i-coupled receptors to promote T cell egress. *Immunity.* 2008; 28:122–133. [PubMed: 18164221]
41. Tough DF, Sprent J, Stephens GL. Measurement of T and B cell turnover with bromodeoxyuridine. *Curr. Protoc. Immunol.* 2007 Chapter 4, Unit 4.7.
42. Wright DE, et al. Cyclophosphamide/granulocyte colony-stimulating factor causes selective mobilization of bone marrow hematopoietic stem cells into the blood after M phase of the cell cycle. *Blood.* 2001; 97:2278–2285. [PubMed: 11290588]
43. Brown C, Blaho V, Loiacono C. Susceptibility to experimental Lyme arthritis correlates with KC and monocyte chemoattractant protein-1 production in joints and requires neutrophil recruitment via CXCR2. *J. Immunol.* 2003; 171:893–901. [PubMed: 12847259]
44. Hammad SM, et al. Blood sphingolipidomics in healthy humans: impact of sample collection methodology. *J. Lipid Res.* 2010; 51:3074–3087. [PubMed: 20660127]
45. Hammad SM, Al Gadban MM, Semler AJ, Klein RL. Sphingosine 1-phosphate distribution in human plasma: associations with lipid profiles. *J. Lipids.* 2012; 2012:180705. [PubMed: 23209911]
46. Min JK, Yoo HS, Lee EY, Lee WJ, Lee YM. Simultaneous quantitative analysis of sphingoid base 1-phosphates in biological samples by o-phthalaldehyde precolumn derivatization after dephosphorylation with alkaline phosphatase. *Anal. Biochem.* 2002; 303:167–175. [PubMed: 11950216]

47. Wolfrum C, Poy MN, Stoffel M. Apolipoprotein M is required for prebeta-HDL formation and cholesterol efflux to HDL and protects against atherosclerosis. *Nat. Med.* 2005; 11:418–422. [PubMed: 15793583]
48. Pino PA, Cardona AE. Isolation of brain and spinal cord mononuclear cells using percoll gradients. *J. Vis. Exp.* 2011 doi:10.3791/2348.

Author Manuscript

Author Manuscript

Author Manuscript

Author Manuscript

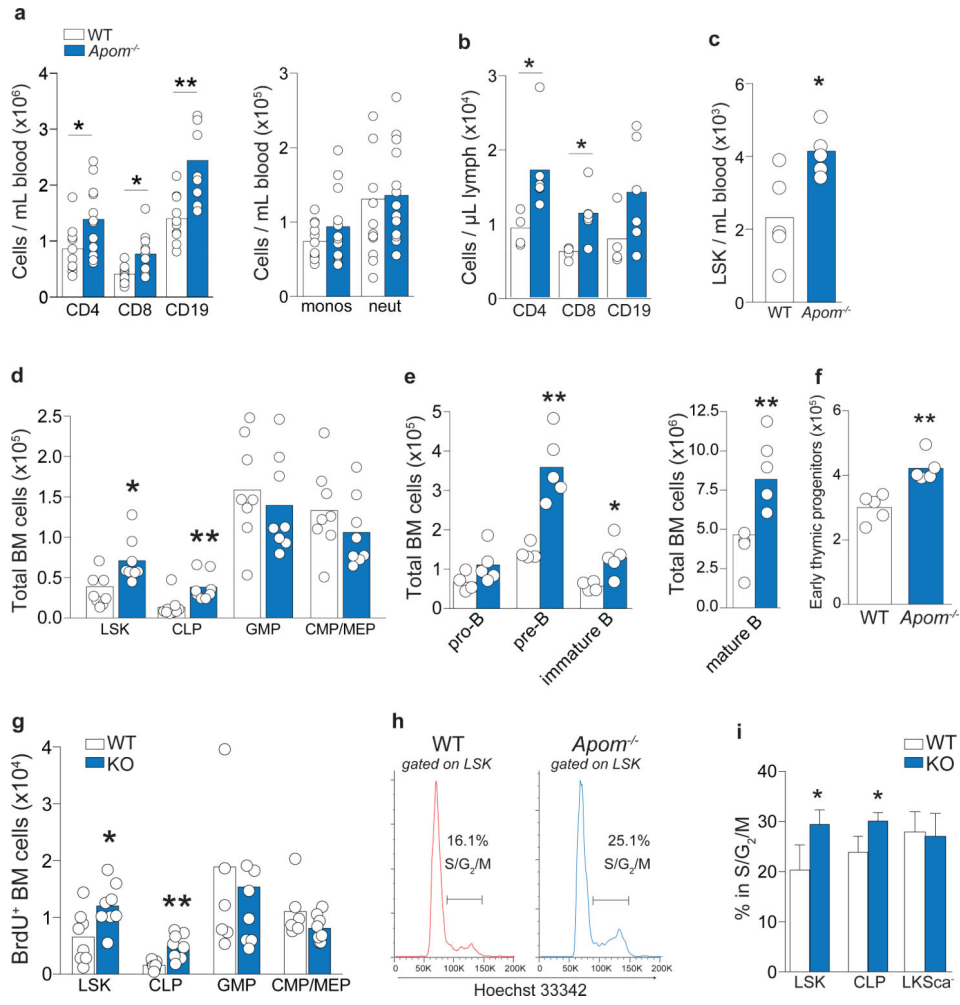


Figure 1. Increased lymphocytes and their progenitors in *Apom*^{-/-} mice
a, CD4 and CD8 T cells, CD19 B cells, monocytes, and neutrophils in blood or **b**, lymph from WT (white) and *Apom*^{-/-} (blue) mice. **c**, LSK cells in blood of WT and *Apom*^{-/-} mice. **d** Stem and progenitor cell populations in bone marrow (BM) of WT and *Apom*^{-/-}. **e**, Pro-pre, immature, and mature B cell populations in BM of WT and *Apom*^{-/-} mice. **f**, Early thymic progenitors (ETP) in thymi of WT and *Apom*^{-/-} mice. **g**, **h**, Proliferation of progenitors in BM of WT and *Apom*^{-/-} mice determined by BrdU incorporation. (**a-g**) Circles indicate values from individual mice and bars represent means. Data are compiled from two (**b, c, e, f**) or four (**a, d, g**) independent experiments. **h**, Representative histograms of Hoechst 33342-stained LSK bone marrow cells from WT and *Apom*^{-/-} mice demonstrating entry into cell cycle. Numbers above bars represent percentage of cells in S/G₂/M phase. **i**, Quantification of cycling LSK, CLP, and LKSc^a subsets in WT and *Apom*^{-/-} mice. Bars represent means ± SD. *n* = 4. Graphs are representative of at least two experiments. **p* < 0.05, ***p* < 0.005 as compared to WT.

Author Manuscript

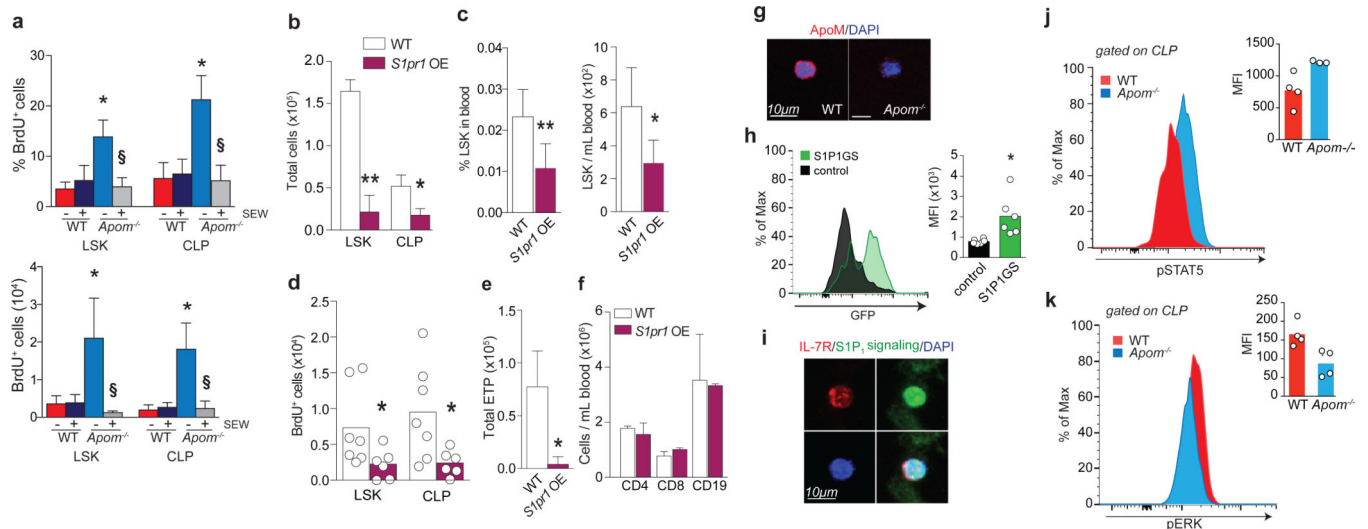


Figure 2. ApoM/ S1P/ S1P₁ signaling suppresses LSK and CLP expansion

a, % BrdU incorporation (left panel) and total BrdU⁺ (right panel) LSK and CLP in WT and *ApoM*^{-/-} BM 24 hours post-treatment with SEW 2871. *n* = 6. **p* < 0.05 versus WT; §*p* < 0.05 versus vehicle-treated control. **b**, LSK and CLP in BM and **c**, percentage and total number of LSK in blood of *S1pr1* OE mice and WT littermates. *S1pr1* OE, *n* = 6; WT, *n* = 7. **d**, BrdU incorporation by BM LSK and CLP of WT and *S1pr1* OE mice. **e**, ETP, or **f**, blood CD4⁺, CD8⁺, and CD19⁺ cells from WT and *S1pr1* OE mice. *S1pr1* OE, *n* = 6; WT, *n* = 7. **g**, Immunofluorescence of ApoM (red) bound to the surface of Lin⁻ Sca1⁺ (LSK and CLP) cells from WT or *ApoM*^{-/-} BM. DAPI nuclear counter stain, blue. **h**, Representative histogram and quantitative median fluorescence intensity (MFI) of GFP expression by CLP from BM of S1P₁ GFP signaling (green) or control (black) mice. **i**, Immunofluorescence of IL-7R (red) expression of GFP (green) by CLP. DAPI nuclear counter stain, blue. **j**, Representative flow cytometry histograms of p-Stat5 and **k**, p-ERK1/2 in WT (red) and *ApoM*^{-/-} (blue) CLPs. MFI of p-Stat5 and p-ERK1/2 in CLP of 3-4 WT or *ApoM*^{-/-} mice are shown in inset. **(d, h-k)** Bars represent means and circles represent values from individual animals. **(b, c, e, f)** Bars represent means ± SD. **p* < 0.05; ***p* < 0.005 versus WT or control. **(a-c, e, f, h, j)** Data are combined from two experiments. **(d)** Data are combined from three experiments. **(g and i)**, Data are representative of at least four experiments.

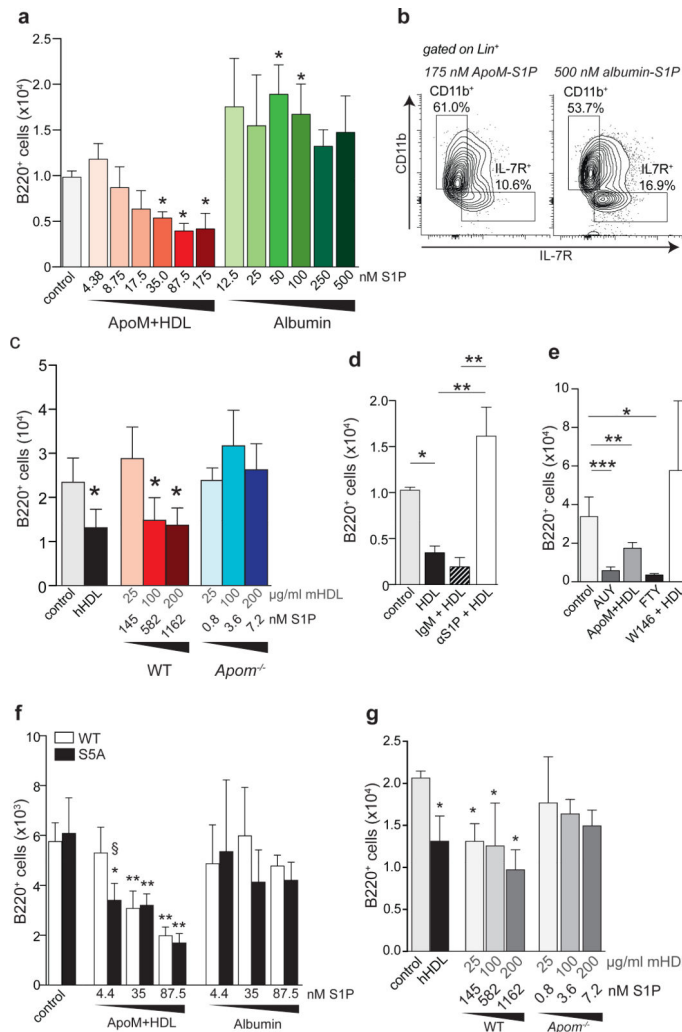


Figure 3. ApoM-S1P activation of S1P₁ suppresses lymphocyte progenitor generation *in vitro*
a, B220⁺ cells generated from WT Lin⁻ BM after incubation with increasing concentrations of ApoM⁺HDL S1P or albumin-S1P. **b**, Representative flow cytometry plots of IL-7R⁺ versus CD11b⁺ cells generated in the presence of 175 nM ApoM-S1P or 500 nM albumin-S1P. **c**, B220⁺ cell numbers generated after culture in the presence of human HDL (hHDL; 100 µg/ml), or increasing concentrations of mouse ApoM⁺HDL (WT) or ApoM⁻HDL (*Apom*^{-/-}). **d**, B220⁺ cells generated after incubation with ApoM⁺HDL (50 µg/mL), ApoM⁺HDL + IgM, or ApoM⁺HDL + αS1P. **e**, B220⁺ cells generated in the presence of vehicle, AUY954 (10 nM), FTY720p (10 nM), 100 µg/ml ApoM⁺HDL, or W146 (100 nM) + 100 µg/ml HDL. **f**, B220⁺ cells generated from WT or S1P₁^{S5A} (S5A) Lin⁻ BM cells after incubation in the presence of increasing concentrations of ApoM⁺HDL-S1P or albumin-S1P. **g**, Number of B220⁺ cells generated from S5A Lin⁻ BM incubated with increasing concentrations of ApoM⁺HDL (WT) or ApoM-HDL (*Apom*^{-/-}). (a-c) *n* = 5; (d, e) *n* = 6 and data are compiled from two independent experiments. (f & g) WT, *n* = 5; S5A, *n* = 3 and data are representative of two experiments. **p* < 0.05; ***p* < 0.005; ****p* < 0.001 versus control or vehicle values. Bars represent mean ± SD.

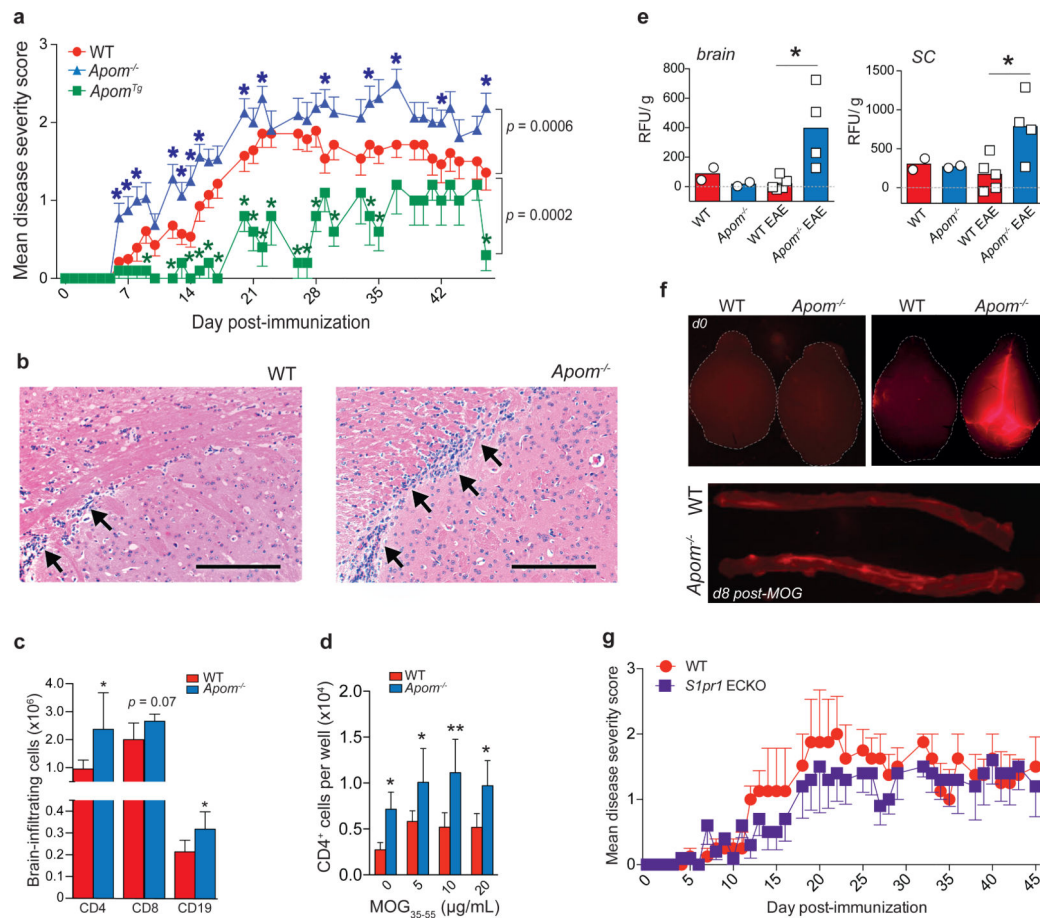


Figure 4. ApoM expression affects EAE disease onset and severity

a, Mean clinical EAE scores of WT, *Apom*^{-/-}, or *Apom*^{Tg} mice. Symbols represent means \pm s.e.m. WT, $n = 14$; *Apom*^{-/-}, $n = 16$; *Apom*^{Tg}, $n = 5$. Data from WT and *Apom*^{-/-} mice are representative of three independent experiments. * $p < 0.05$ compared to WT value as determined by Mann-Whitney *U*-test. **b**, Representative photomicrographs of hematoxylin and eosin staining of brains from WT or *Apom*^{-/-} mice at d16 post-MOG₃₅₋₅₅ immunization. Scale bar, 100 μ m. **c**, Numbers of brain-infiltrating CD4, CD8, and CD19 cells from CNS of WT and *Apom*^{-/-} EAE mice at day 24 post-immunization. **d**, Number of CD4 T cells from splenocytes of MOG₃₅₋₅₅-immunized WT or *Apom*^{-/-} EAE mice following *ex vivo* restimulation with increasing concentrations of MOG₃₅₋₅₅ peptide. (c & d) Bars represent means \pm SD. * $p < 0.05$, ** $p < 0.01$ compared to WT. Experiments were performed at least twice with cells from $n = 5$ / arm. **e**, Quantification of TMR-dextran fluorescence in brain and spinal cord after 16h of circulation in WT or *Apom*^{-/-} mice at d0 or d8 post-MOG₃₅₋₅₅ immunization. Bars represent means and symbols represent values from individual mice. Data are combined from two experiments. **f**, Representative photographs of whole brains or spinal cords quantified in (e). **g**, Mean clinical EAE scores of *S1pr1* ECKO and WT littermates. Symbols represent means \pm s.e.m. $n = 5$ per arm and data are representative of two experiments performed.